Distinct focal adhesion protein modules control different aspects of mechanotransduction

DOI:
10.1242/jcs.195362

Document Version
Accepted author manuscript

Citation for published version (APA):
Stutchbury, B., Atherton, P., Tsang, R., Wang, D-Y., & Ballestrem, C. (2017). Distinct focal adhesion protein modules control different aspects of mechanotransduction. *Journal of Cell Science*, *130*(9), 1612-1624. https://doi.org/10.1242/jcs.195362

Published in:
Journal of Cell Science

Distinct focal adhesion protein modules control different aspects of mechanotransduction

Keywords: Vinculin, Talin, Paxillin, FAK, Mechanotransduction, Focal Adhesion

Authors/Affiliations:

Ben Stutchbury, Paul Atherton, Ricky Tsang, De-Yao Wang and Christoph Ballestrem.

Wellcome Trust Centre for Cell-Matrix Research, University of Manchester, Manchester, M13 9PT, England, UK

Correspondence should be addressed to Christoph Ballestrem.

Email: christoph.ballestrem@manchester.ac.uk

Journal of Cell Science • Advance article

JCS Advance Online Article. Posted on 16 March 2017

Summary Statement

Mechanotransduction is a fundamental process carried out by almost every cell. This paper shows that focal adhesions are composed of functional protein modules, which control distinct aspects of mechanotransduction.

Abstract

Focal adhesions (FAs) are macromolecular complexes that regulate cell adhesion and mechanotransduction. Using fluorescence recovery after photobleaching (FRAP) and fluorescence loss after photoactivation (FLAP), we found that the mobility of core FA proteins correlates with protein function. Structural proteins such as tensin, talin and vinculin are significantly less mobile in FAs than signaling proteins such as FAK and paxillin. The mobilities of the structural proteins are directly influenced by substrate stiffness, suggesting they are involved in sensing the rigidity of the extracellular environment. The turnover rates of FAK and paxillin as well as kindlin2 are not influenced by substrate stiffness. By using specific Src and FAK kinase inhibitors, we reveal that force-sensing by vinculin occurs independently of FAK and paxillin phosphorylation. However, this phosphorylation is required for downstream, Rac1-driven cellular processes, such as protrusion and cell migration. Overall, we show that the FA is composed of different functional modules that separately control mechanosensing and the cellular mechano-response.

Introduction

Fundamental cellular processes such as adhesion and migration require precise communication between cells and their environment (Geiger et al., 2001). Focal adhesions (FAs) are major sites of cell-extracellular matrix (ECM) crosstalk (Yamada and Geiger, 1997). Here, the integrin transmembrane receptors connect ECM proteins to the cytoplasmic FA plaque complex, providing a link to the contractile actomyosin machinery (Hynes, 2002). While the overall molecular architecture of FAs has been established (Kanchanawong et al., 2010; Liu et al., 2015), much less is known about the dynamic processes that occur within FAs, and their functional relevance to mechanotransduction, the conversion of a mechanical signal into a cellular response.

Talin, vinculin and tensin are three FA structural proteins that provide a physical link between the integrins and the actin cytoskeleton (Atherton et al., 2016; Calderwood et al., 2013). Talin binds to and activates integrins and is essential for cell adhesion and spreading (Atherton et al., 2015), while absence of vinculin compromises FA function and force transduction (Dumbauld et al., 2013; Xu et al., 1998). Tensin, depending on the isoform can vary in its localization pattern (Clarke et al., 2015). While tensin2 appeared predominantly in FAs, tensin3 was almost exclusively in fibrillar adhesions (FBs). Tensin1 localizes to both FAs and FBs (Clarke et al., 2015). In spite of these findings, little is known about the activation and regulation of tensin. Talin and vinculin activation requires tension-dependent conformational changes (Atherton et al., 2015; Carisey et al., 2013; del Rio et al., 2009; Hirata et al., 2014a), suggesting they are involved in sensing force-generated signals from the environment. When active, talin and vinculin bind both to each other and to the actomyosin machinery, leading to the maturation and stabilization of the FA, a process that is dependent on actomyosin tension (Humphries et al., 2007). There is evidence to suggest that the actin-crosslinker α-actinin may also be required for tension-dependent FA maturation (Roca-Cusachs et al., 2013). This could be due to the transmission of forces through α-actinin (Roca-Cusachs et al., 2013), or via the establishment of an actin stress-fiber template (Oakes et al., 2012).

Kindlin2, FAK and paxillin also contribute to adhesion regulation and mechanotransduction. Kindlin2 is essential for integrin activation and is involved in recruitment of paxillin (Theodosiou et al., 2016). FAK and paxillin phosphorylation is increased on rigid substrates (Bae et al., 2014). Additionally, FAK phosphorylation is required for cells to respond to substrate stiffness during cell spreading (Swaminathan et al., 2016). FAK forms a complex with Src kinase in FAs (Parsons, 2003), which also seems to play a key role in mechanotransduction as Src kinase activity (Sai et al., 1999) and subsequent FAK phosphorylation (Wang et al., 2001) are required for the cellular response to cyclic

stretching. Phosphorylation, mainly driven by the FAK-Src complex, also dictates the localization of paxillin at cell-ECM adhesions (Zaidel-Bar et al., 2007). A phosphomimetic form of paxillin, where two key tyrosine residues (Y31 and Y118) were mutated to glutamate (Y2E), preferentially localized to newly formed FXs, whereas the phospho-null mutation (Y2F) localized to fibrillar adhesions. It is not known, however, whether these proteins are involved in the initial sensing of substrate stiffness, or are required to orchestrate the cellular response.

FA proteins do not remain stationary; rather, they are continually turned over from the complex (Lele et al., 2006). Here, we used the photokinetic microscopy techniques fluorescence recovery after photobleaching (FRAP) and fluorescence loss after photoactivation (FLAP) to measure how the dynamics of 12 core FA proteins vary within the FA. We found that adhesion proteins can be separated into distinct 'modules' based on their turnover, which is representative of protein function. The turnover rates of the 'structural module' proteins talin, vinculin and tensin are stabilized by increased extracellular substrate stiffness and appear to be important in mechanosensing. This response is not seen with FAK and paxillin, two proteins in the 'signaling module'. Furthermore, we show that FAK and paxillin have a role in directing the cellular response by controlling lamellipodial protrusions and cell migration.

These results highlight the distinct roles played by different FA protein modules, allowing a cell to sense and respond to extracellular mechanical signals. Both the structural and signaling protein modules are critical for mechanosensitive cellular processes such as coordinated cell migration.

Results

Differential mobility of FA proteins.

A large number of proteins are implicated in the regulation of FAs, but little is known about their dynamic behavior. We analyzed the mobility of 12 GFP-tagged FA proteins using FRAP (Figure 1A; Movie S1). Two parameters, the half-time (t½) of recovery and the mobile fraction (F_M), were assessed as indicators of protein mobility (Carisey et al., 2011).

FRAP experiments revealed a wide distribution in the t½ of different FA proteins (Figure 1B). We found tensin1 (t½ = 59.0 s) and talin (t½ = 49.4 s) to have the slowest turnover, followed by vinculin (t½ = 39.8 s), α-actinin (t½ = 29.6 s), ILK (t½ = 29.1 s), α-Parvin (t½ = 26.0 s), kindlin2 (t½ = 23.3 s), paxillin (t½ = 15.7 s), p130Cas (t½ = 14.4 s), VASP (t½ = 11.1 s), FAK (t½ = 9.9 s) and zyxin (t½ = 9.4 s) (Figure 1B). The statistical analysis of t½ FRAP indicates that these proteins can be broadly split into three groups. Tensin, talin and vinculin are the slowest; α-actinin, ILK, α-Parvin and kindlin2 make up the intermediate group; and the remaining proteins constitute the most rapidly cycling group of proteins (Figure 1B). Analyzing mobile fractions (F_M) showed talin and tensin to have the lowest F_M (48.4 % and 57.3 %), followed by the other FA proteins analyzed (F_M between 60-80%) (Figure S1A).

To compare the dynamics of the cytoplasmic plaque proteins with transmembrane, ECM-bound integrins, we used FRAP to study the turnover of GFP-β1-integrin. Initial observations showed a short t½ FRAP of 19.4 s, suggesting a surprisingly fast turnover. However, the low F_M (36.5%) indicated a high immobile fraction (Figure 1C). Analyzing line profiles of fluorescence intensities during the course of recovery showed that GFP-β1-integrin only recovered to the levels observed in the background membrane areas outside FAs, which constitutes diffuse GFP-β1-integrin (approximately 30% of the total initial intensity found in FAs) (Figure 1D). This suggests the presence of two populations of integrins in FAs; one population that is tightly engaged with the ECM and therefore less mobile than a second highly mobile population, with a similar mobility to unliganded, presumably inactive, integrins in other areas of the membrane.

Taken together, these results reveal the differential dynamics of distinct groups of FA proteins, suggesting a modular organization of proteins with a similar function within the FA.

Structural, but not signaling, proteins modify their turnover in response to extracellular stiffness

FLAP is a complementary method to FRAP for measuring protein turnover (Atherton et al., 2015). FLAP experiments using PA(GFP)-tagged talin, vinculin, FAK and paxillin, with mCherry-zyxin used as a FA marker showed a similar protein turnover pattern as FRAP, with

talin and vinculin displaying significantly higher t½ compared to FAK and paxillin (Figure S1B, C). We found no correlation between initial fluorescence intensity post-photoactivation, (relating to protein expression level), and the rate of turnover, demonstrating that protein expression levels did not influence the rate of protein turnover (Figure S1D). This method was used instead of FRAP in subsequent experiments because the analysis of the positive fluorescence signal after photoactivation was less variable and more sensitive.

Of the 12 proteins analyzed previously, we chose tensin1, talin, vinculin, α-actinin, kindlin2, paxillin and FAK to examine further. Vinculin and talin are known mechanosensors and FAK and paxillin are important signaling components involved in regulating FA dynamics and mechanotransduction (Bae et al., 2014; Dumbauld et al., 2013; Humphries et al., 2007; Webb et al., 2004; Zaidel-Bar et al., 2007). The roles of the other 3 proteins in mechanotransduction are not well established. To test whether the mechanical properties of the ECM affect protein dynamics, we performed FLAP experiments with NIH3T3 cells cultured on FN-coated intermediate (~8 kPa) and stiff (~100 kPa) polyacrylamide (PAA) gel substrates and glass (~1GPa) (Figure 2A). The rigidities chosen for the PAA gels are within the physiological range (~8 kPa ~ muscle, ~100 kPa ~ collagenous bone) (Engler et al., 2006). Consistent with previous findings, cells on the three substrates spread well and displayed FAs that increased in size with substrate stiffness (Figure S2A, B) (Han et al., 2012; Pelham and Wang, 1997). Analyzing turnover rates revealed that the t½ for talin, vinculin and tensin significantly increased with substrate stiffness (Figure 2A, B, S2C). Conversely, the dynamics of FAK, paxillin and kindlin2 were unaffected (Figure 2A, B, S2C). Interestingly kindlin2, while not sensitive to forces, showed a different post-activation pattern than that of FAK and paxillin. Fractions of activated PAGFP-paxillin and FAK that were not bound to FAs diffused rapidly away from adhesion sites; however, those of PAGFP-kindlin2 produced a halo around adhesions which seemed to be associated with the membrane (Figure S2D). For α-actinin, we found no difference in turnover between soft and stiff PAA gels (Figure 2A, B, S2C). There was a very small, albeit significant, decrease in mobility between 8 kPa and glass which puts forward the possibility that α-actinin is somewhat sensitive to ECM stiffness in larger force ranges. However since the changes are extremely low in comparison to tensin, talin and vinculin, the latter appear to be the main mechanosensitive proteins of those analyzed.

Overall, these results demonstrate that the turnover of proteins linking integrins to the actin cytoskeleton (vinculin, talin and tensin) is directly influenced by the physical properties of the ECM. Substrate stiffness had no influence on the turnover rates of paxillin, FAK and kindlin2 which appear to associate more transiently with FAs. α-actinin sits between these groups in both rate of turnover and sensitivity to ECM stiffness. The data suggest a modular

composition of FAs with the mobile behavior of protein subsets responding differently when encountering environments of different rigidities.

Phosphorylation state and active vinculin do not affect the dynamics of FAK and paxillin

In order to investigate the molecular mechanisms of mechanical activation in more detail, we focused on talin, vinculin, FAK and paxillin. The activities of vinculin and talin are influenced by the application of forces and constitutively active forms have significantly reduced turnovers compared to WT (Atherton et al., 2015; Cohen et al., 2006; Humphries et al., 2007). FAK and paxillin, however, are predominantly regulated by tyrosine phosphorylation. To analyze the effect of phosphorylation on protein turnover, we performed FLAP with FAK and paxillin, mutated at crucial tyrosine residues (Figure 3A).

Interestingly, for paxillin, neither phosphomimetic (Y2E) nor phospho-null (Y2F) mutations had any effect on the mobility of the protein in FAs (Figure 3B-D). Similarly, for FAK, neither mutating its autophosphorylation (Y397F) site nor a kinase-dead (K454R) form, which significantly reduces autophosphorylation (Schaller et al., 1999), had any impact on turnover (Figure 3 B-D).

Using FLAP, we have previously shown that talin has a significantly reduced mobility in the presence of a constitutively active form of vinculin (vinT12) (Figure S3A and Atherton et al., 2015). We found here that the co-expression of vinT12 had no effect on the turnover of FAK and paxillin (Figure S3A-C).

Together, these data demonstrate that the dynamic exchange of FAK and paxillin are not affected by their phosphorylation state or vinculin activity; however, talin is stabilized by active vinculin. Again, results support a modular organization within FAs whereby the activity of one set of proteins can affect the mobility of similar proteins within the same module, but has no influence on the dynamics of others in separate modules.

FAK and paxillin phosphorylation in mechanotransduction

Results so far indicate that the dynamics of paxillin and FAK are unaffected by substrate stiffness, phosphorylation or vinculin activity. Therefore, we investigated whether they contribute to mechanotransduction via an alternative mechanism, such as altered phosphorylation. To this end, we analyzed the ratio of total paxillin to phospho-paxillin (pY118) and the ratio of total paxillin to phospho-FAK (pY397) using immunofluorescence of cells on FN-coated PAA gels or glass (Figure S3D). We found that the percentage of the cell area that is composed of pY118-paxilin or pY397-FAK positive FAs (area fraction) increases with substrate stiffness (Figure 4A). Interestingly, the ratio of paxillin:pY118-paxillin and

paxillin:pY397-FAK did not change significantly (Figure 4B), indicating that substrate stiffness affects the overall amount of phosphorylated paxillin and FAK localized to FAs, but not the relative composition.

Earlier results suggested that the dynamics of only FA proteins linking integrins to the actin cytoskeleton change their dynamics in response to ECM stiffness. We next explored whether the varying levels of phosphorylated FAK and paxillin present at FAs in cells on different substrates contributes to the dynamics of these proteins. We inhibited phosphorylation by treating cells with specific FAK and Src kinase inhibitors (FAKi – AZ13256675, Srci – AZD0530) (Figure S4A). These inhibitors have been extensively characterized and lead to a strong inhibition of FAK and paxillin phosphorylation in the FA (Horton et al., 2016, Figure S4A). Similar results were obtained using an alternative FAK inhibitor (PF573,228) (data not shown). FRAP analysis showed that FAKi and Srci treatment had no effect on the turnover of vinculin or FAK, compared to the DMSO control (Figure S4B).

To test whether FAK and paxillin phosphorylation contributes to mechanosensing, we used FLAP to examine vinculin and tensin mobility on the PAA gels, following treatment with FAKi and Srci. For vinculin, inhibitor-treated cells showed the same previously seen pattern of reduced dynamic exchange as the substrate rigidity increased from 8 kPa to 100 kPa and from 100 kPa to glass (~1 GPa) (Figure 4C, D). Conversely, upon inhibition of FAK and Src activity, the turnover of tensin was no longer sensitive to ECM stiffness, with no significant difference in t½ FLAP between the substrates (Figure 4C, D).

These results indicate that mechanosensing by vinculin and tensin occurs via different mechanisms. Vinculin is mechanosensitive irrespective of FAK and Src kinase activity. Surprisingly, tensin shows the opposite behavior and is no longer mechanosensitive when FAK and Src are inhibited.

FAK and Src kinase activity influence FA dynamics

Our previous results showed that FA morphology and phosphorylation of FAK and paxillin at FAs are both influenced by substrate stiffness (Figure S2, 4A). Therefore, we wanted to test the impact of FAK and paxillin phosphorylation on FA formation and turnover. Inhibiting FAK and Src activity (combined treatment with FAKi and Srci) led to a reduction in the number of small dot-like FXs at the cell periphery compared to DMSO-treated control cells, but their formation was not completely abolished (Figure 5A). Furthermore, inhibitor-treated cells had more mature FAs, leading to an increase in mean FA size (Figure 5A-B).

To analyze FA dynamics in real time, we acquired time-lapse recordings of cells transfected with GFP-paxillin, with or without inhibitors. In DMSO-treated cells, FAs clearly matured from

FXs that localized along the entire edge of protruding lamellipodia. In contrast, cells treated with the combination of FAKi and Srci had a reduced number of FXs, and many FAs appeared to mature from complexes at the base of prominent filopodia (Figure 5C, 6B; Movie S2). Interestingly, these cells displayed extremely stable FAs, which persisted for much longer than the dynamic adhesions in control cells (Figure 5C; Movie S2). Cells treated with the FAKi alone displayed a phenotype in-between control cells and cells treated with both inhibitors (Figure 5C).

Cells treated with FAKi and Srci appeared to form fewer FXs and more large FAs. Conversely, treatment with the Rho-kinase (ROCK) inhibitor Y-27632 leads to the disassembly of mature, tension-dependent FAs, but tension-independent FXs are still present (Ballestrem et al., 2001). Therefore, we hypothesized that cells lacking FAK, Src and ROCK activity will not be able to form any cell-matrix adhesion structures. To our surprise, NIH3T3 cells pre-treated in suspension with FAKi, Srci and Y-27632 were still able to spread and form FXs at the cell periphery. These were positive for vinculin and paxillin (Figure S4C), but contained no tyrosine-phosphorylated paxillin (Figure 5D).

Together, these results suggest that adhesion complexes are extremely robust structures. Furthermore, although important for FA turnover, tyrosine phosphorylation of FAK and paxillin is not necessary for initial FX formation.

FAK and Src kinase activity are required for lamellipodial protrusions, migration and cell spreading.

The preceding experiments indicated that there is little, if any, role for FAK and paxillin phosphorylation in FA formation, but that they are involved in adhesion disassembly. Therefore, we hypothesized that the major role of their phosphorylation may lie in the coordination of cellular protrusions. Tracking the cell edge dynamics of NIH3T3 cells expressing RFP-Lifeact using the QuimP plugin for imageJ (Tyson et al., 2010) revealed that control (DMSO-treated) cells formed large, polarized protrusions, typically associated with 2D directional cell migration. FAKi treated cells also formed lamellipodia, but these appeared as multiple small and disorganized protrusions (Figure 6A; Movie S3). In contrast, cells treated with FAKi + Srci together formed no lamellipodia and were largely stationary, but had a large number of prominent filopodia at the cell edge (Figure 6A, B; Movie S3).

These defects in polarized protrusion formation after drug treatment also translated into defects in polarized, two-dimensional migration. DMSO-treated cells plated on 10 µm wide fibronectin (FN) stripes (which forces cells to adopt an elongated shape, thus assisting cell polarization (Doyle et al., 2009)) migrated readily along the stripes. Conversely, cells treated

with FAKi showed a significant reduction in cell migration, which was completely blocked by treatment with FAKi + Srci (Figure 6C and Figure S4D).

Both lamellipodial protrusion and migration are Rac1 dependent processes (Ridley, 2011). To further analyze the role of FAK and Src mediated phosphorylation in Rac1-driven cellular functions, we performed cell spreading assays, a process also known to be driven by Rac (Price et al., 1998) While FAKi treatment of NIH3T3 cells barely affected long-term cell spreading (150 minutes), the process was significantly slower than for control cells. This effect was more pronounced using both FAKi and Srci (Figure 6D and Figure S4E).

From these data, we conclude that phosphorylation of FAK and paxillin is vital to generate Rac1 driven cellular processes such as lamellipodial protrusions, which are critical for polarized cell migration and spreading.

Src-mediated tyrosine phosphorylation of FAK and paxillin has no impact on cellular traction forces.

Coordinated cell motility and environmental stiffness sensing requires force exertion by the cell onto the matrix (Plotnikov et al., 2012). To explore whether the observed defects in cell migration and spreading could be due to a reduction in these forces, we measured the traction forces exerted by cells following treatment with FAKi and Srci. This treatment did not lead to any change in the traction stress applied by cells to the substrate (Figure 6E). Therefore, although vital for initiating cellular protrusions, FAK and paxillin phosphorylation does not contribute to the generation of traction forces required to sense ECM stiffness and to pull the cell body forward during migration.

Discussion

FAs are composed of a complex network of proteins that are integral for ECM stiffness sensing, cell adhesion and migration (Geiger et al., 2001). We have shown that FA proteins are organized into functional modules, and that these modules are each responsible for regulating distinct aspects of mechanotransduction.

Here, we classify the FA proteins that have been previously shown to link ECM-bound integrins to the actin cytoskeleton (including talin (Calderwood et al., 1999; Zhang et al., 2008), vinculin (Case et al., 2015; Menkel et al., 1994), and tensin (Haynie, 2014)) as belonging to a 'structural module'. FA proteins known to be involved in adhesion-based signalling such as FAK (Mitra et al., 2005),and paxillin (Deakin and Turner, 2008) belong to a 'signalling module'. Some proteins, such as kindlin2 and a-actinin, have been shown to have alternative roles, and belong to an intermediate module (Otey and Carpen, 2004; Roca-Cusachs et al., 2013; Theodosiou et al., 2016). In line with their roles as structural proteins with the FA, those proteins in the structural module have the slowest turnover, as measured by FRAP, whereas the signalling module proteins have a very fast turnover, suggesting a much more transient residency time within the adhesion (Figure 1B).

Interestingly, the structural module proteins (talin, vinculin and tensin), but not the signalling module proteins (FAK and paxillin), change their turnover in response to ECM stiffness. This suggests that it is those proteins that are involved in linking integrins to the actin cytoskeleton that are directly involved in sensing ECM stiffness. Our results showing that FAK- and Src-mediated phosphorylation within adhesions is required for protrusion (Figure 6A), migration (Figure 6C) and spreading (Figure 6D), all of which are Rac1-dependent events (Ridley, 2011) that are also affected by substrate stiffness (Lo et al., 2000; Plotnikov et al., 2012; Swaminathan et al., 2016), suggest that these signalling module proteins are involved in generating the intracellular signalling events driving these phenomena. Therefore, the process of mechanotransduction requires the co-operation of both modules to function correctly: the structural proteins are involved in directly sensing mechanical stimuli (mechanosensing), whereas the signaling module proteins are involved in generating the intracellular signaling events in response (mechanosignaling) (Figure 7).

The recent finding that FAK Y397 phosphorylation is required for stiffness-dependent cell spreading agrees with this model (Swaminathan et al., 2016). We propose that these cells are still mechanosensitive but are deficient in mechanosignaling. Similarly, perturbing either of these modules blocks polarized cell motility as has been shown with knockout cells, mutants or drugs that compromise talin and vinculin function (Atherton et al., 2015; Carisey

et al., 2013), or FAK and paxillin function (Ilic et al., 1995; Petit et al., 2000; Swaminathan et al., 2016; Webb et al., 2004).

Differences in protein turnover rates reflect distinct function in cells.

The observed differences in turnover rates between FA proteins were striking (Figure 1). Lele et al (2008) proposed that the turnover rate of an FA protein may, in part, depend on its number of interaction partners. It appears, however, that the function of the protein has a greater influence. Integrins have the lowest mobility, but can be subdivided into two populations, a more stable ligand binding fraction and a highly mobile fraction that diffuses in the membrane (Figure 1C, D). This is supported by super-resolution microscopy that found reduced movement of integrins within FAs (Rossier et al., 2012).

After the slowly turned over structural proteins, there appears to be a module of proteins with intermediary turnover rates contains actin-binding proteins including α-actinin and the ILK–PINCH-parvin complex. These proteins may be more involved in crosslinking the actin cytoskeleton, rather than linking integrins to the actomyosin machinery. However, more work will be required to analyze this subset of proteins further. As well as containing the highly mobile signaling proteins (FAK, paxillin and p130Cas), the third module also comprises proteins known to regulate actin polymerization (e.g. zyxin and VASP) (Beckerle, 1998; Hoffman et al., 2006). Proteins in the latter group localize to actin filament termini and are involved in actin organization and polymerization (Beckerle, 1998; Drees et al., 1999), rather than being an integral part of the mechanical structure between integrins and actin.

Interestingly, classifying FA proteins according to their dynamic behavior correlates well with the compartments identified using super-resolution microscopy (Kanchanawong et al., 2010; Liu et al., 2015): (i) the ‘integrin signaling layer’ (containing FAK and paxillin), (ii) the ‘force transduction layer’ (talin and vinculin) and (iii) the ‘actin regulatory layer’ (zyxin, VASP and α-actinin). According to our data, proteins residing within these individual layers have very similar rates of turnover. One interesting exception is α-actinin, whose slow turnover is likely due to its role as an actin cross-linker (Otey and Carpen, 2004), as well as its direct association with β-integrin (Roca-Cusachs et al., 2013).

Kindlin2, whilst turned over rapidly, showed a unique pattern of mobility. In contrast to other proteins, much of the protein diffused along the plasma membrane starting from the initially photoactivated pool of the FA structure (Figure S2D). These findings are in line with kindlin2 bearing a pleckstrin-homology (PH) domain that binds phosphoinositides and is involved in recruiting proteins to the plasma membrane (Liu et al., 2011).

The relationship between protein dynamics and mechanosensing.

Mechanical forces are thought to contribute to the activation of both talin and vinculin (del Rio et al., 2009; Hirata et al., 2014b; Yao et al., 2014). Previously, we have shown that the turnover of talin and vinculin reflects their activation state (Atherton et al., 2015; Carisey et al., 2013). Our observation that the turnover rates of talin, vinculin and tensin decreased with increasing ECM stiffness (Figure 2), suggests that these proteins are more active on rigid substrates. Increasing ECM stiffness leads to elevated Rho activity (Paszek et al., 2005), therefore it is possible that this in turn, through a downstream increase of actomyosin tension, leads to increased activation of talin and vinculin in adhesion sites. Indeed, it has been shown using a talin tension sensor construct, that the amount of tension across talin is modified by substrate stiffness and that vinculin is required for the maximal tension to be applied through talin at FAs (Austen et al., 2015; Kumar et al., 2016).

Tensin1 is present within both FAs and FBs (Clark et al., 2010). Our findings suggest that, within FAs under normal conditions, tensin1 is exposed to forces in a similar manner to talin and vinculin, and possibly acts as a mechanosensor via an analogous mechanism**.**

Interestingly, the above-mentioned mechanosensitive proteins differ from α-actinin in that α-actinin does not modify its turnover in response to different substrate stiffness on PAA gels (Figure 2). Therefore, while on one hand α-actinin may be part of the clutch model, whereby talin and vinculin follow actin retrograde flow out of FAs, controlling the transmission of actomyosin tension through FAs (Hu et al., 2007; Thievessen et al., 2013), we propose that it belongs to a different, actin-binding module distinct from the mechanically activated integrin-talin-vinculin complex, in line with the super-resolution microscopy findings showing α-actinin in an actin-binding layer.

Crosstalk between the modules and its role in mechanosensing

Interestingly, constitutively active vinculin does not influence the turnover of FAK or paxillin, proteins in the ‘signaling module’ (Figure S3). This is surprising, given that both of these proteins remain present at FAs after removal of intracellular tension using either blebbistatin or Rho-kinase inhibition, when co-expressed with vinT12 (Carisey et al., 2013).

The phosphorylation of the signalling module proteins FAK and paxillin is critical for cell motility (Figure 6C) (Mitra et al., 2005; Subauste et al., 2004). The overall amount of phosphorylated FAK and paxillin that localized to FAs increased with substrate stiffness (Figure 4A). This builds on previous biochemical data, which found the whole-cell levels of phospho-FAK and paxillin increased on rigid substrates (Bae et al., 2014). Importantly, inhibiting phosphorylation using a combination of FAKi and Srci did not affect the ability of

vinculin to modify its turnover in response to ECM stiffness (Figure 4C, D). Similarly, in marked contrast to the well-documented roles for vinculin and talin in generating cellular traction forces (Atherton et al., 2015; Dumbauld et al., 2013; Thievessen et al., 2013), which are crucial for mechanosensing (Plotnikov et al., 2012), we find that FAK and Src inhibition has no effect on traction force generation (Figure 6E). This suggests that this module is not directly involved in sensing environmental mechanical cues. Rather, it appears to control the downstream response to these signals through the activation of Rac1, which is essential for cell edge protrusions and migration (Ballestrem et al., 2001) (Figure 6).

It has been suggested that tension-dependent paxillin phosphorylation has a role in vinculin recruitment to FAs (Case et al., 2015; Pasapera et al., 2010). However, we observed vinculin in FXs in the absence of both intracellular tension and tyrosine-phosphorylated paxillin (Figure 5D and S4C), suggesting that vinculin can be recruited to FXs by several mechanisms.

It is interesting to note that tensin1 lost the ability to modify its turnover in response to ECM stiffness after drug treatment (Figure 4C, D). Tensin binds to the NPxY motif of the β-integrin cytoplasmic tail at the same site as talin, and phosphorylation of the tyrosine motif by Src has been shown to greatly reduce the affinity for talin, thus leading to an increase in tensin recruitment (McCleverty et al., 2007). Additionally, we found that the turnover of tensin on glass is increased after drug treatment ($t_{½}$ = 89.7 s (drugs) vs 123.8 s (no drugs)) (compare Figure 4D with Figure 2B). Therefore, tensin may be insensitive to ECM stiffness changes after FAKi and Srci treatment due to perturbation to its recruitment under these conditions.

Together, these findings suggest that a complex feedback mechanism exists between the FA protein modules. Although they themselves do not appear to be directly sensitive to ECM stiffness, proteins in the signaling module of the FA still appear to have a role in influencing the recruitment and mechanosensitive function of FA structural proteins.

Our findings shed further light on the modular organization of FAs and how separate modules contribute to mechanotransduction in distinct ways. Understanding precisely how these FA protein modules communicate with one another requires further research and would be an extremely interesting line of enquiry.

Materials and methods

Antibodies and reagents

Primary antibodies and dilutions used were: anti-vinculin (clone hVIN-1 - Sigma) (1:500); anti-paxillin (clone 349 – Milipore) (1:400); anti-paxillin pY118 (clone 44-722G – Life Technologies) (1:400); anti-FAK pY397 (clone 141-9 – Life Technologies) (1:400) and anti-pY (clone 4G10 - Milipore) (1:250). Secondary antibodies conjugated to DyLight-488 or -594 were all from Jackson ImmunoResearch Laboratories (both 1:500). Texas-Red-X- (1:500) and Alexa Fluor 647-conjugated (1:200) phalloidin were from Life Technologies.

The FAK inhibitor (FAKi – AZ13256675) and Src inhibitor (Srci – AZD0530) were obtained from Astra Zeneca, available from the pharmacology toolbox (http://openinnovation.astrazeneca.com/what-we-offer/pharmacology-toolbox/). Y-27632 dihydrochloride was obtained from Tocris Bioscience.

Microscopy

Immunofluorescence microscopy and FRAP experiments were carried out using a Delta Vision (Applied Precision) microscope using a 60x/1.42 Plan-Apochromat (immunofluorescence) or 100x/1.40 Uplan S Apochromat (FRAP) objective and a Sedat Quad filter set (Chroma 86000v2*)*, with images collected using a Coolsnap HQ (Photometrics) camera.

FLAP experiments, time lapse recordings and actin retrograde flow measurements were acquired using a CSU-X1 spinning disc confocal (Yokagowa) on a Zeiss Axio-Observer Z1 microscope with a 60x/1.40 oil Plan-Apochromat objective, Evolve EMCCD camera (Photometrics) and motorised XYZ stage (ASI). The 405 nm, 488 nm and 561 nm lasers were controlled using an Acousto-optical tunable filter through the laserstack (Intelligent Imaging Innovations (3i)).

For all constructs, we analysed cells with low to intermediate expression levels. Protein expression level had no effect on the rate of protein turnover (Figure S1D).

Cell migration experiments were performed using an AS MDW live cell imaging system (Leica) using a 10x/0.30 HC Plan Fluotar objective. The system was controlled using Image Pro 6.3 by Media Cybernetics LtD. Cells were maintained at 37°C and 5% CO_2. Images were collected using a Coolsnap HQ CCD camera (Photometrics).

Cell lines and transfection

NIH3T3 fibroblasts were cultured at 37°C in Dulbecco's Modified Eagle Medium (DMEM) (Sigma), supplemented with 10% (vol/vol) Fetal Calf Serum (FCS) (Lonza), 1% (vol/vol) non-essential amino acids and 2 mM L-glutamine (both Sigma), and transfected using Lipofectamine reagent and Plus reagent, according to manufacturer's instructions (Life Technologies). Cells were plated on glass-bottomed dishes (IBL) coated with 10 µg/ml bovine plasma fibronectin (FN) (Sigma). For live cell imaging experiments, the cells were transferred to carbonate-free Ham's F-12 media supplemented with L-glutamine, 25 mM HEPES, penicillin-streptomycin (all Sigma) and 2% FCS. Starting solutions of FAKi and Srci were diluted in DMSO (3 mM) and Y-27632 was diluted in water (100 mM).

Immunofluorescence microscopy

Cells were fixed with 4% (wt/vol) PFA and permeabilized with 0.5% (vol/vol) Triton-X (both Sigma-Aldrich). Antibodies were diluted in 1% BSA (Sigma-Aldrich) and added to the cells for 1 hour.

Images were acquired on the Delta Vison system (above) and processed using the FIJI-ImageJ software (version 1.48u). To analyse FA size and area fraction, images were bandpass filtered and background was subtracted using a rolling ball. FAs were thresholded manually and particle analysis between 0.1-10 μm^2 was used to analyse the average adhesion size for each cell.

For ratio imaging of pY118-paxillin/pY397-FAK:total paxillin, images of co-immunostained cells were taken with the same exposure time between channels. FA images were processed as above. The same threshold was used in both the paxillin and pY118-paxillin/pY397-FAK channels. The mean intensity of every adhesion was measured in both channel using particle analysis, and the ratio of pY118-Pax/pY397-FAK:Pax was calculated for all adhesions in the cell.

Flilpodia were quantified using the FiloDetect MatLab script, developed and made freely available by Theodore Perkins' research group, University of Ottawa (Nilufar et al., 2013).

Y-27632 experiments

NIH3T3 cells were trypsinised and suspended in 2 ml supplemented DMEM containing 3 µM FAKi + 3 µM Srci + 50 µM Y-27632, or an equivalent volume of DMSO for 1 hour. These concentrations and treatment times are sufficient for maximal FAK and Src inhibition (Horton

et al., 2016). Cells were plated on FN-coated coverslips for 4 hr prior to fixation and staining. Images were acquired with the DeltaVision system (above).

Polyacrylamide gel preparation

FN-coated PAA gels (6% (~8 kPa) or 25% (~100 kPa) of gel diluted from 30% Protogel in PBS, 37.5:1 fixed ratio of acrylamide:bis-acrylamide; EC-890, National Diagnostics) were prepared in 35 mm glass bottomed dishes (IBL) from previously published methods, with modifications (Pelham and Wang, 1998; Zhang et al., 2013). The FN coating density was equivalent between PAA gels and glass.

The stiffness of the 6% (8.760 ± 0.209 kPa) and 25% (113.188 ± 8.04 kPa) PAA gels were measured with a CellHesion Atomic Force Microscope (Nanowizard, CellHesion 200; JPK Instruments, Berlin, Germany) with tip-less cantilevers (NP-O10, Bruker AFM Probes), modified by attaching 10 mm diameter polystyrene beads (PPS-10.0, Kisker).

Live cell imaging

Fluorescence recovery after photobleaching (FRAP)

Transfected NIH3T3 fibroblasts were incubated overnight at 37ºC. The cells were placed in the microscope chamber at 37ºC for 1 hour prior to imaging, to ensure they were in equilibrium. For cells treated with FAKi and Srci, media containing 3 µM FAKi, 3 µM FAKi + 3 µM Srci or an equivalent volume of DMSO were added to the cells for 1 hour..

Images were acquired using the Delta Vision system (above). 5 peripheral, mature FAs per cell were selected and photobleaching was achieved with a 7.5 ms burst of the 488 nm laser at 100% power, used to bleach a 2 µm diameter circle within the FAs. Softworks software was used to capture three images prior to photobleaching and then one image every 10 s for 5 min post-bleach. Movies were analysed using Softworks inbuilt photokinetics analysis and MATLAB, with a script developed in house, as described previously (Carisey et al., 2011; Humphries et al., 2007).

Fluorescence loss after photoactivation (FLAP)

NIH3T3 fibroblasts were co-transfected with the required photoactivatable (PA)GFP tagged DNA constructs and an mCherry-tagged FA marker protein (mCh-zyxin, unless otherwise specified). The cells were incubated overnight at 37ºC. The medium was replaced and the cells were placed in the microscope chamber at 37ºC for 1 hour.

Cells were imaged using the CSU-X1 spinning disc confocal system. Approximately 5 peripheral, mature FAs were photoactivated per cell with a 5 ms burst of a 405 nm laser at

100% power. Slidebook software was used to capture three images prior to photoactivation and images were then taken every 10 s for 3-5 min post-photoactivation.

Movies were analysed using MATLAB with a script developed in house, as described previously (Atherton et al., 2015).

FAKi and Srci experiments

NIH3T3 cells were co-transfected with GFP-paxillin or YFP-dSH2 and plated on fibronectin coated glass bottomed dishes (IBL). Cells were treated as described above for 1 hour prior to fixation. Cells were imaged using the CSU-X1 spinning disc confocal system.

For time lapse recordings, the media was replaced 1 hour prior to imaging with supplemented DMEM containing 3 µM FAKi, 3 µM FAKi + 3 µM Srci or an equivalent volume of DMSO. Images were acquired every 2 minutes for 90 minutes. Cell membrane protrusion was analysed using the QuimP11b toolbox for ImageJ, kindly provided by Till Bretschneider and Richard Tyson (University of Warwick, Coventry, UK, (Tyson et al., 2010)).

Migration

Polydimethylsiloxane (PDMS) stamps were generated by coating a glass mask (10 µm stripes) with PDMS (10:1 weight ratio of base:curing agent) and heating to 60ºC for 2 hours. The PDMS stamps were coated with 50 µg/ml FN for 1 hour at room temperature and placed on a glass coverslip for 1 hour.

NIH3T3 cells were plated on the patterned coverslips for 1 hour at 37ºC. Unattached cells were washed away with PBS and the media was replaced with supplemented DMEM containing 25 mM HEPES as well as 3 µM FAKi, 3 µM FAKi + Srci or an equivalent volume of DMSO. Cells were incubated for 1 hour prior to imaging. Images were acquired every 10 minutes for 16 hours using the AS MDW live cell imaging system (above). Cell migration was measured using the Manual Tracking plugin, and analysed using the chemotaxis and migration tool for FIJI-ImageJ (Ibidi).

Spreading

NIH3T3 cells were trypsinised and suspended in 1 ml supplemented DMEM containing 3 µM FAKi, 3 µM FAKi + Srci or an equivalent volume of DMSO for 1 hour. Treated cells were plated on FN-coated coverslips and fixed after the indicated times and stained for actin. Images were acquired using an AxioObserver Z1 microscope with a 10x objective and a 565 nm LED. Cell area was measured manually using FIJI-ImageJ software.

Traction force microscopy

NIH3T3 cells were transfected with GFP-paxillin and plated on FN coated ~8 kPa PAA gels containing 4% (vol/vol) FluoSpheres carboxylate-modified microspheres (F8810, red fluorescent (580/605) (Thermo Fisher). Cells were treated with 3 µM FAKi, 3 µM FAKi + Srci or an equivalent volume of DMSO for 1 hour prior to imaging. Traction force images were acquired on the CSU-X1 spinning disc confocal system (above), and analysed as previously described (Atherton et al., 2015).

Statistical analysis

Graphing and statistical analysis were performed using GraphPad Prism 6 software.

When comparing means, the D'Agostino-Pearson test was used to assess the normality of the data to determine the appropriate statistical tests to use.

Author Contributions

B.S., P.A. and R.T. designed and conducted the experiments and analyzed the data. B.S. and P.A. performed photoactivation experiments and experiments using FAKi and Srci. R.T. performed FRAP experiments and P.A ran the traction force experiments. D.Y.W designed the protocols for PAA gel preparation and traction force microscopy. C.B., B.S., P.S and R.T. conceived the ideas; C.B. and B.S. wrote the manuscript with contributions from R.T. and P.A. C.B. supervised and directed the project.

Acknowledgements

C.B. acknowledges the Biotechnology and Biological Sciences Research Council (BBSRC) and Wellcome Trust for funding of this project. The CB laboratory is part of the Wellcome Trust Centre for Cell-Matrix Research, University of Manchester, which is supported by core funding from the Wellcome Trust (grant number 088785/Z/09/Z). B.S. is supported by Wellcome Trust (099734/Z/12/Z). R.T. was supported by a BBSRC DTP studentship. P.A. is funded by BBSRC (BB/J012254/1) and Bioventus; The Bioimaging Facility microscopes were purchased with grants from BBSRC, Wellcome Trust, and the University of Manchester Strategic Fund. Special thanks to Simon T. Barry from AstraZeneca for providing the FAK inhibitor and Professor David Critchley, Professor Martin Humphries and Janet Askari for critical reading of the manuscript. We thank the staff of the Bioimaging facility at the University of Manchester, in particular Dr Peter March and Dr Egor Zindy for their help with imaging and analysis. Dr Kristian Franze for his help with traction force microscopy analysis and Till Bretschneider for providing the QuimP11b software.

Competing interests

No competing interests declared.

References

Atherton, P., B. Stutchbury, D. Jethwa, and C. Ballestrem. 2016. Mechanosensitive components of integrin adhesions: Role of vinculin. *Exp Cell Res*. 343:21-27.

Atherton, P., B. Stutchbury, D.Y. Wang, D. Jethwa, R. Tsang, E. Meiler-Rodriguez, P. Wang, N. Bate, R. Zent, I.L. Barsukov, B.T. Goult, D.R. Critchley, and C. Ballestrem. 2015. Vinculin controls talin engagement with the actomyosin machinery. *Nat Commun*. 6:10038.

Austen, K., P. Ringer, A. Mehlich, A. Chrostek-Grashoff, C. Kluger, C. Klingner, B. Sabass, R. Zent, M. Rief, and C. Grashoff. 2015. Extracellular rigidity sensing by talin isoform-specific mechanical linkages. *Nat Cell Biol*.

Bae, Y.H., K.L. Mui, B.Y. Hsu, S.L. Liu, A. Cretu, Z. Razinia, T. Xu, E. Pure, and R.K. Assoian. 2014. A FAK-Cas-Rac-Lamellipodin Signaling Module Transduces Extracellular Matrix Stiffness into Mechanosensitive Cell Cycling. *Sci Signal*. 7:ra57.

Ballestrem, C., B. Hinz, B.A. Imhof, and B. Wehrle-Haller. 2001. Marching at the front and dragging behind: differential alphaVbeta3-integrin turnover regulates focal adhesion behavior. *J Cell Biol*. 155:1319-1332.

Beckerle, M.C. 1998. Spatial control of actin filament assembly: lessons from Listeria. *Cell*. 95:741-748.

Calderwood, D.A., I.D. Campbell, and D.R. Critchley. 2013. Talins and kindlins: partners in integrin-mediated adhesion. *Nature Reviews Molecular Cell Biology*. 14:503-517.

Calderwood, D.A., R. Zent, R. Grant, D.J. Rees, R.O. Hynes, and M.H. Ginsberg. 1999. The Talin head domain binds to integrin beta subunit cytoplasmic tails and regulates integrin activation. *J Biol Chem*. 274:28071-28074.

Carisey, A., M. Stroud, R. Tsang, and C. Ballestrem. 2011. Fluorescence recovery after photobleaching. *Methods Mol Biol*. 769:387-402.

Carisey, A., R. Tsang, Alexandra M. Greiner, N. Nijenhuis, N. Heath, A. Nazgiewicz, R. Kemkemer, B. Derby, J. Spatz, and C. Ballestrem. 2013. Vinculin Regulates the Recruitment and Release of Core Focal Adhesion Proteins in a Force-Dependent Manner. *Current Biology*. 23:271-281.

Case, L.B., M.A. Baird, G. Shtengel, S.L. Campbell, H.F. Hess, M.W. Davidson, and C.M. Waterman. 2015. Molecular mechanism of vinculin activation and nanoscale spatial organization in focal adhesions. *Nat Cell Biol*.

Clark, K., J.D. Howe, C.E. Pullar, J.A. Green, V.V. Artym, K.M. Yamada, and D.R. Critchley. 2010. Tensin 2 modulates cell contractility in 3D collagen gels through the RhoGAP DLC1. *J Cell Biochem*. 109:808-817.

Clarke, J.H., M.L. Giudici, J.E. Burke, R.L. Williams, D.J. Maloney, J. Marugan, and R.F. Irvine. 2015. The function of phosphatidylinositol 5-phosphate 4-kinase gamma (PI5P4Kgamma) explored using a specific inhibitor that targets the PI5P-binding site. *Biochem J*. 466:359-367.

Cohen, D.M., B. Kutscher, H. Chen, D.B. Murphy, and S.W. Craig. 2006. A conformational switch in vinculin drives formation and dynamics of a talin-vinculin complex at focal adhesions. *J Biol Chem*. 281:16006-16015.

Deakin, N.O., and C.E. Turner. 2008. Paxillin comes of age. *J Cell Sci*. 121:2435-2444.

del Rio, A., R. Perez-Jimenez, R. Liu, P. Roca-Cusachs, J.M. Fernandez, and M.P. Sheetz. 2009. Stretching single talin rod molecules activates vinculin binding. *Science*. 323:638-641.

Drees, B.E., K.M. Andrews, and M.C. Beckerle. 1999. Molecular dissection of zyxin function reveals its involvement in cell motility. *J Cell Biol*. 147:1549-1560.

Dumbauld, D.W., T.T. Lee, A. Singh, J. Scrimgeour, C.A. Gersbach, E.A. Zamir, J. Fu, C.S. Chen, J.E. Curtis, S.W. Craig, and A.J. Garcia. 2013. How vinculin regulates force transmission. *Proc Natl Acad Sci U S A*. 110:9788-9793.

Engler, A.J., S. Sen, H.L. Sweeney, and D.E. Discher. 2006. Matrix Elasticity Directs Stem Cell Lineage Specification. *Cell*. 126:677-689.

Geiger, B., A. Bershadsky, R. Pankov, and K.M. Yamada. 2001. Transmembrane crosstalk between the extracellular matrix and the cytoskeleton. *Nat Rev Mol Cell Biol*. 2:793-805.

Han, S.J., K.S. Bielawski, L.H. Ting, M.L. Rodriguez, and N.J. Sniadecki. 2012. Decoupling substrate stiffness, spread area, and micropost density: a close spatial relationship between traction forces and focal adhesions. *Biophys J*. 103:640-648.

Haynie, D.T. 2014. Molecular physiology of the tensin brotherhood of integrin adaptor proteins. *Proteins*. 82:1113-1127.

Hirata, H., K.H. Chiam, C.T. Lim, and M. Sokabe. 2014a. Actin flow and talin dynamics govern rigidity sensing in actin-integrin linkage through talin extension. *J R Soc Interface*. 11.

Hirata, H., H. Tatsumi, C.T. Lim, and M. Sokabe. 2014b. Force-dependent vinculin binding to talin in live cells: a crucial step in anchoring the actin cytoskeleton to focal adhesions. *Am J Physiol Cell Physiol*.
Hoffman, L.M., C.C. Jensen, S. Kloeker, C.L. Wang, M. Yoshigi, and M.C. Beckerle. 2006. Genetic ablation of zyxin causes Mena/VASP mislocalization, increased motility, and deficits in actin remodeling. *J Cell Biol*. 172:771-782.
Horton, E.R., J.D. Humphries, B. Stutchbury, G. Jacquemet, C. Ballestrem, S.T. Barry, and M.J. Humphries. 2016. Modulation of FAK and Src adhesion signaling occurs independently of adhesion complex composition. *J Cell Biol*. 212:349-364.
Hu, K., L. Ji, K.T. Applegate, G. Danuser, and C.M. Waterman-Storer. 2007. Differential transmission of actin motion within focal adhesions. *Science*. 315:111-115.
Humphries, J.D., P. Wang, C. Streuli, B. Geiger, M.J. Humphries, and C. Ballestrem. 2007. Vinculin controls focal adhesion formation by direct interactions with talin and actin. *The Journal of Cell Biology*. 179:1043-1057.
Hynes, R.O. 2002. Integrins: bidirectional, allosteric signaling machines. *Cell*. 110:673-687.
Ilic, D., Y. Furuta, S. Kanazawa, N. Takeda, K. Sobue, N. Nakatsuji, S. Nomura, J. Fujimoto, M. Okada, and T. Yamamoto. 1995. Reduced cell motility and enhanced focal adhesion contact formation in cells from FAK-deficient mice. *Nature*. 377:539-544.
Kanchanawong, P., G. Shtengel, A.M. Pasapera, E.B. Ramko, M.W. Davidson, H.F. Hess, and C.M. Waterman. 2010. Nanoscale architecture of integrin-based cell adhesions. *Nature*. 468:580-584.
Kumar, A., M. Ouyang, K. Van den Dries, E.J. McGhee, K. Tanaka, M.D. Anderson, A. Groisman, B.T. Goult, K.I. Anderson, and M.A. Schwartz. 2016. Talin tension sensor reveals novel features of focal adhesion force transmission and mechanosensitivity. *J Cell Biol*. 213:371-383.
Lele, T.P., J. Pendse, S. Kumar, M. Salanga, J. Karavitis, and D.E. Ingber. 2006. Mechanical forces alter zyxin unbinding kinetics within focal adhesions of living cells. *J Cell Physiol*. 207:187-194.
Lele, T.P., C.K. Thodeti, J. Pendse, and D.E. Ingber. 2008. Investigating complexity of protein–protein interactions in focal adhesions. *Biochemical and Biophysical Research Communications*. 369:929-934.
Liu, J., K. Fukuda, Z. Xu, Y.Q. Ma, J. Hirbawi, X. Mao, C. Wu, E.F. Plow, and J. Qin. 2011. Structural basis of phosphoinositide binding to kindlin-2 protein pleckstrin homology domain in regulating integrin activation. *J Biol Chem*. 286:43334-43342.
Liu, J., Y. Wang, W.I. Goh, H. Goh, M.A. Baird, S. Ruehland, S. Teo, N. Bate, D.R. Critchley, M.W. Davidson, and P. Kanchanawong. 2015. Talin determines the nanoscale architecture of focal adhesions. *Proc Natl Acad Sci U S A*.
Lo, C.M., H.B. Wang, M. Dembo, and Y.L. Wang. 2000. Cell movement is guided by the rigidity of the substrate. *Biophys J*. 79:144-152.
McCleverty, C.J., D.C. Lin, and R.C. Liddington. 2007. Structure of the PTB domain of tensin1 and a model for its recruitment to fibrillar adhesions. *Protein Sci*. 16:1223-1229.
Menkel, A.R., M. Kroemker, P. Bubeck, M. Ronsiek, G. Nikolai, and B.M. Jockusch. 1994. Characterization of an F-actin-binding domain in the cytoskeletal protein vinculin. *J Cell Biol*. 126:1231-1240.
Mitra, S.K., D.A. Hanson, and D.D. Schlaepfer. 2005. Focal adhesion kinase: in command and control of cell motility. *Nat Rev Mol Cell Biol*. 6:56-68.
Nilufar, S., A.A. Morrow, J.M. Lee, and T.J. Perkins. 2013. FiloDetect: automatic detection of filopodia from fluorescence microscopy images. *BMC Syst Biol*. 7:66.
Oakes, P.W., Y. Beckham, J. Stricker, and M.L. Gardel. 2012. Tension is required but not sufficient for focal adhesion maturation without a stress fiber template. *The Journal of Cell Biology*. 196:363-374.
Otey, C.A., and O. Carpen. 2004. Alpha-actinin revisited: a fresh look at an old player. *Cell Motil Cytoskeleton*. 58:104-111.
Parsons, J.T. 2003. Focal adhesion kinase: the first ten years. *J Cell Sci*. 116:1409-1416.
Pasapera, A.M., I.C. Schneider, E. Rericha, D.D. Schlaepfer, and C.M. Waterman. 2010. Myosin II activity regulates vinculin recruitment to focal adhesions through FAK-mediated paxillin phosphorylation. *The Journal of Cell Biology*. 188:877-890.
Paszek, M.J., N. Zahir, K.R. Johnson, J.N. Lakins, G.I. Rozenberg, A. Gefen, C.A. Reinhart-King, S.S. Margulies, M. Dembo, D. Boettiger, D.A. Hammer, and V.M. Weaver. 2005. Tensional homeostasis and the malignant phenotype. *Cancer Cell*. 8:241-254.

Pelham, R.J., Jr., and Y. Wang. 1997. Cell locomotion and focal adhesions are regulated by substrate flexibility. *Proc Natl Acad Sci U S A*. 94:13661-13665.
Pelham, R.J., Jr., and Y.L. Wang. 1998. Cell locomotion and focal adhesions are regulated by the mechanical properties of the substrate. *Biol Bull*. 194:348-349; discussion 349-350.
Petit, V., B. Boyer, D. Lentz, C.E. Turner, J.P. Thiery, and A.M. Valles. 2000. Phosphorylation of tyrosine residues 31 and 118 on paxillin regulates cell migration through an association with CRK in NBT-II cells. *J Cell Biol*. 148:957-970.
Plotnikov, Sergey V., Ana M. Pasapera, B. Sabass, and Clare M. Waterman. 2012. Force Fluctuations within Focal Adhesions Mediate ECM-Rigidity Sensing to Guide Directed Cell Migration. *Cell*. 151:1513-1527.
Price, L.S., J. Leng, M.A. Schwartz, and G.M. Bokoch. 1998. Activation of Rac and Cdc42 by integrins mediates cell spreading. *Mol Biol Cell*. 9:1863-1871.
Ridley, A.J. 2011. Life at the leading edge. *Cell*. 145:1012-1022.
Roca-Cusachs, P., A. del Rio, E. Puklin-Faucher, N.C. Gauthier, N. Biais, and M.P. Sheetz. 2013. Integrin-dependent force transmission to the extracellular matrix by alpha-actinin triggers adhesion maturation. *Proc Natl Acad Sci U S A*. 110:E1361-1370.
Rossier, O., V. Octeau, J.-B. Sibarita, C. Leduc, B. Tessier, D. Nair, V. Gatterdam, O. Destaing, C. Albigès-Rizo, R. Tampé, L. Cognet, D. Choquet, B. Lounis, and G. Giannone. 2012. Integrins β1 and β3 exhibit distinct dynamic nanoscale organizations inside focal adhesions. *Nature Cell Biology*. 14:1057-1067.
Sai, X., K. Naruse, and M. Sokabe. 1999. Activation of pp60(src) is critical for stretch-induced orienting response in fibroblasts. *J Cell Sci*. 112 (Pt 9):1365-1373.
Schaller, M.D., J.D. Hildebrand, and J.T. Parsons. 1999. Complex formation with focal adhesion kinase: A mechanism to regulate activity and subcellular localization of Src kinases. *Mol Biol Cell*. 10:3489-3505.
Subauste, M.C., O. Pertz, E.D. Adamson, C.E. Turner, S. Junger, and K.M. Hahn. 2004. Vinculin modulation of paxillin-FAK interactions regulates ERK to control survival and motility. *J Cell Biol*. 165:371-381.
Swaminathan, V., R.S. Fischer, and C.M. Waterman. 2016. The FAK-Arp2/3 interaction promotes leading edge advance and haptosensing by coupling nascent adhesions to lamellipodia actin. *Mol Biol Cell*.
Theodosiou, M., M. Widmaier, R.T. Bottcher, E. Rognoni, M. Veelders, M. Bharadwaj, A. Lambacher, K. Austen, D.J. Muller, R. Zent, and R. Fassler. 2016. Kindlin-2 cooperates with talin to activate integrins and induces cell spreading by directly binding paxillin. *Elife*. 5.
Thievessen, I., P.M. Thompson, S. Berlemont, K.M. Plevock, S.V. Plotnikov, A. Zemljic-Harpf, R.S. Ross, M.W. Davidson, G. Danuser, S.L. Campbell, and C.M. Waterman. 2013. Vinculin-actin interaction couples actin retrograde flow to focal adhesions, but is dispensable for focal adhesion growth. *The Journal of Cell Biology*. 202:163-177.
Tyson, R.A., D.B.A. Epstein, K.I. Anderson, and T. Bretschneider. 2010. High Resolution Tracking of Cell Membrane Dynamics in Moving Cells: an Electrifying Approach. *Math Model Nat Pheno*. 5:34-55.
Wang, J.G., M. Miyazu, E. Matsushita, M. Sokabe, and K. Naruse. 2001. Uniaxial cyclic stretch induces focal adhesion kinase (FAK) tyrosine phosphorylation followed by mitogen-activated protein kinase (MAPK) activation. *Biochem Biophys Res Commun*. 288:356-361.
Webb, D.J., K. Donais, L.A. Whitmore, S.M. Thomas, C.E. Turner, J.T. Parsons, and A.F. Horwitz. 2004. FAK-Src signalling through paxillin, ERK and MLCK regulates adhesion disassembly. *Nat Cell Biol*. 6:154-161.
Xu, W., H. Baribault, and E.D. Adamson. 1998. Vinculin knockout results in heart and brain defects during embryonic development. *Development*. 125:327-337.
Yamada, K.M., and B. Geiger. 1997. Molecular interactions in cell adhesion complexes. *Curr Opin Cell Biol*. 9:76-85.
Yao, M., B.T. Goult, H. Chen, P. Cong, M.P. Sheetz, and J. Yan. 2014. Mechanical activation of vinculin binding to talin locks talin in an unfolded conformation. *Sci Rep*. 4:4610.
Zaidel-Bar, R., R. Milo, Z. Kam, and B. Geiger. 2007. A paxillin tyrosine phosphorylation switch regulates the assembly and form of cell-matrix adhesions. *J Cell Sci*. 120:137-148.
Zhang, J., W.H. Guo, A. Rape, and Y.L. Wang. 2013. Micropatterning cell adhesion on polyacrylamide hydrogels. *Methods Mol Biol*. 1066:147-156.
Zhang, X., G. Jiang, Y. Cai, S.J. Monkley, D.R. Critchley, and M.P. Sheetz. 2008. Talin depletion reveals independence of initial cell spreading from integrin activation and traction. *Nature Cell Biology*. 10:1062-1068.

Figures

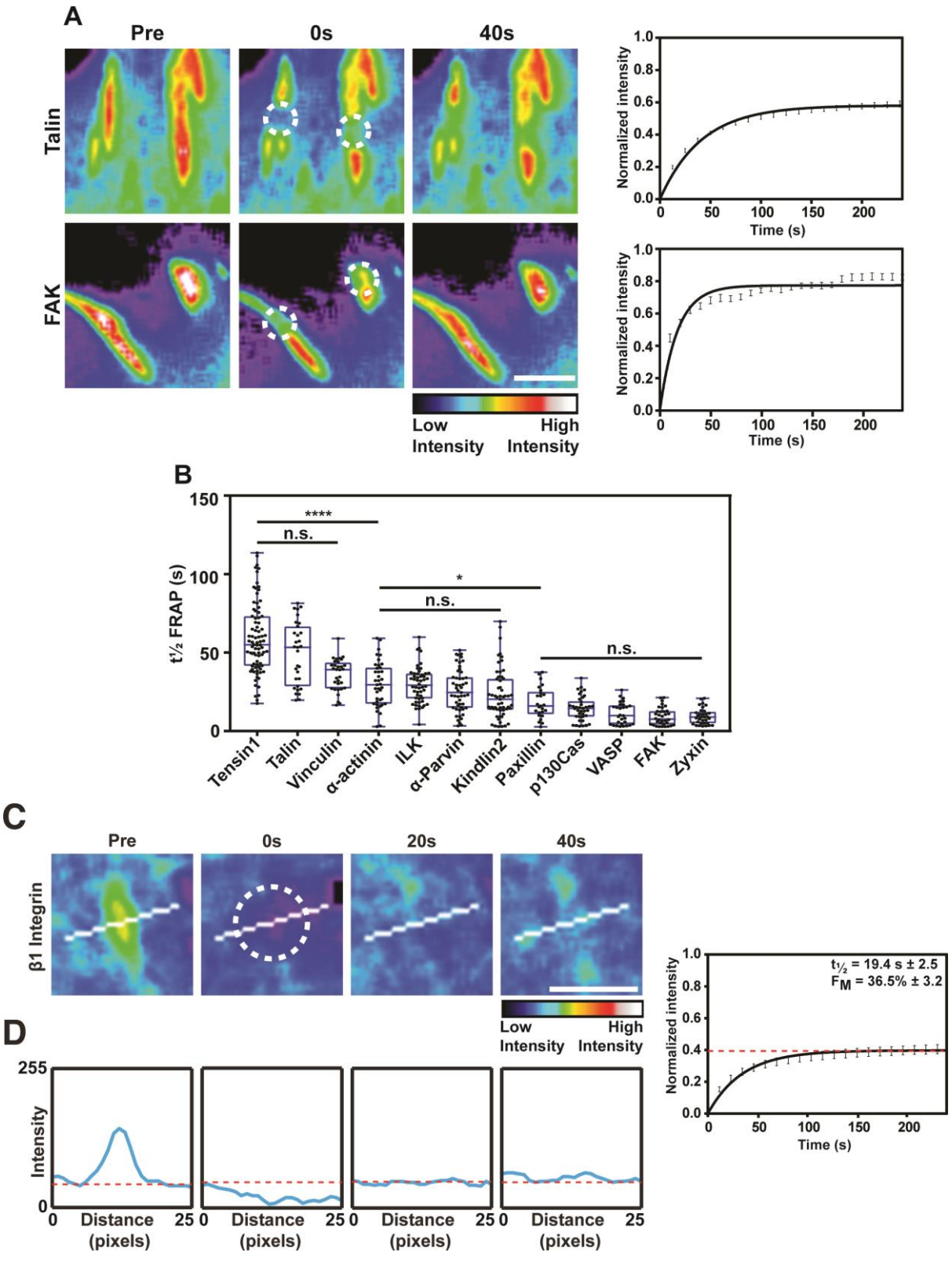

Figure 1. Differential FA protein turnover in FAs.

A. Representative time-lapse images showing FRAP of NIH3T3 cells transfected with GFP-tagged talin and FAK. Targeted FAs are indicated by encircled regions. Images are presented in a color intensity scale. Graphs show the mean fluorescence recovery curves for all recorded FAs, error bars are SEM. Scale bar = 5 µm. **B.** Mean t½ FRAP values for the indicated FA proteins in NIH3T3 cells. n = 23-83 FAs. Kruskal-Wallis with Dunn's multiple comparisons test, n.s. = no significant difference, * = $p < 0.05$, **** = $p < 0.0001$. **C.** Representative time-lapse panels showing FRAP of GFP-β1-integrin. Graph shows the average curve fits of all recorded FAs (n = 20), error bars are SEM. White line across FA indicates the position of line profile plots (below). Scale bar = 5 µm. **D.** Representative line profile plots of GFP-β1-integrin. Blue line represents the fluorescence intensity across the line and red dashed line indicates background fluorescence. Note that the fluorescence intensity of the photobleached FA falls below the background fluorescence at time 0 s and only recovers to background levels at 40 s.

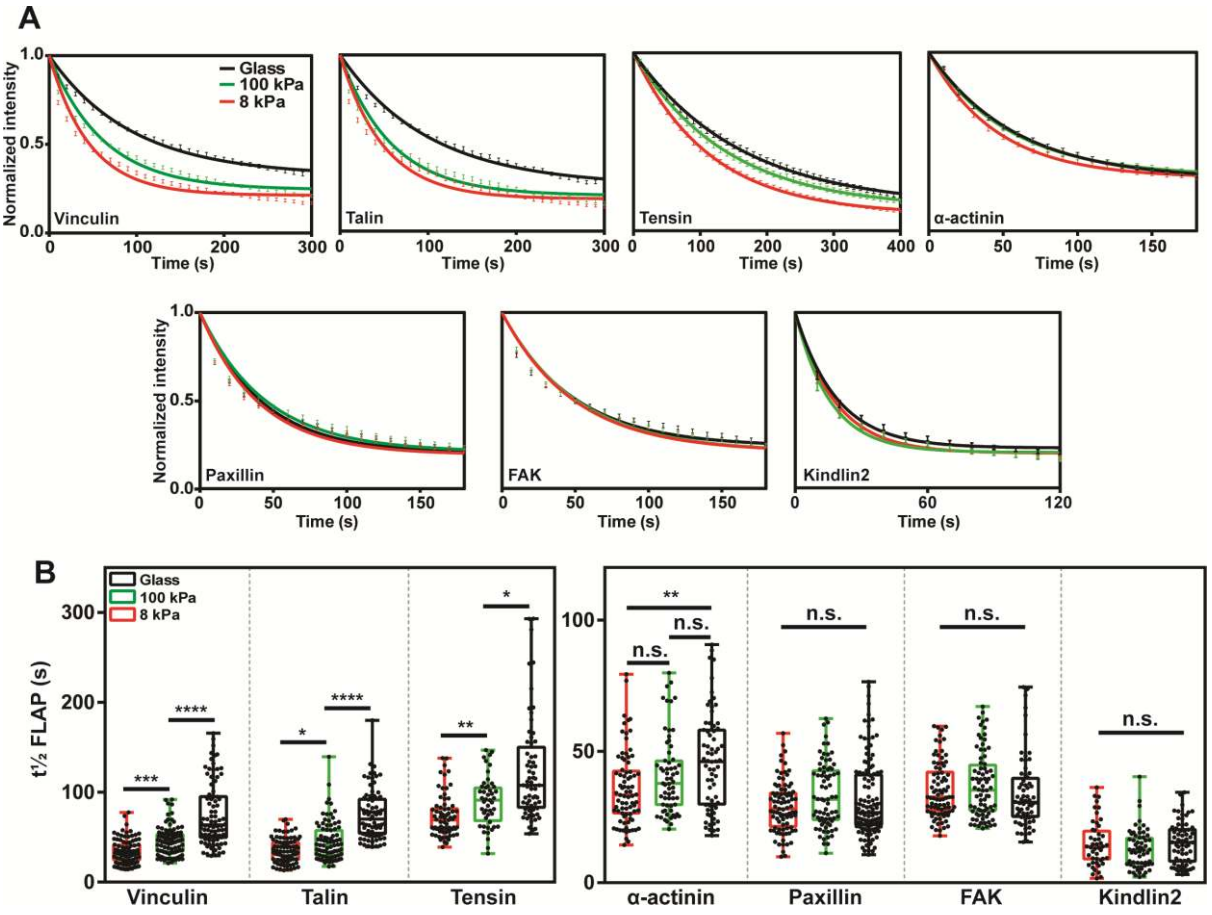

Figure 2. Extracellular stiffness differentially modulates the turnover rates of several FA proteins.

A. FLAP curves of experiments performed in NIH3T3 cells plated on FN-coated 8 kPa and 100 kPa polyacrylamide (PAA) gels and glass. **B.** t½ FLAP graph showing that the turnover rates of talin, vinculin and tensin are stabilized in a step-wise manner as substrate stiffness increases. α-actinin is partially stabilized by increased substrate stiffness, while the dynamics of FAK, paxillin and kindlin2 are unaffected. Data are pooled from 3 independent repeats, n = 47-118 FAs, Kruskal-Wallis with Dunn's multiple comparisons test, n.s. = no significant difference, * = $p < 0.05$, *** = $p < 0.001$, **** = $p < 0.0001$.

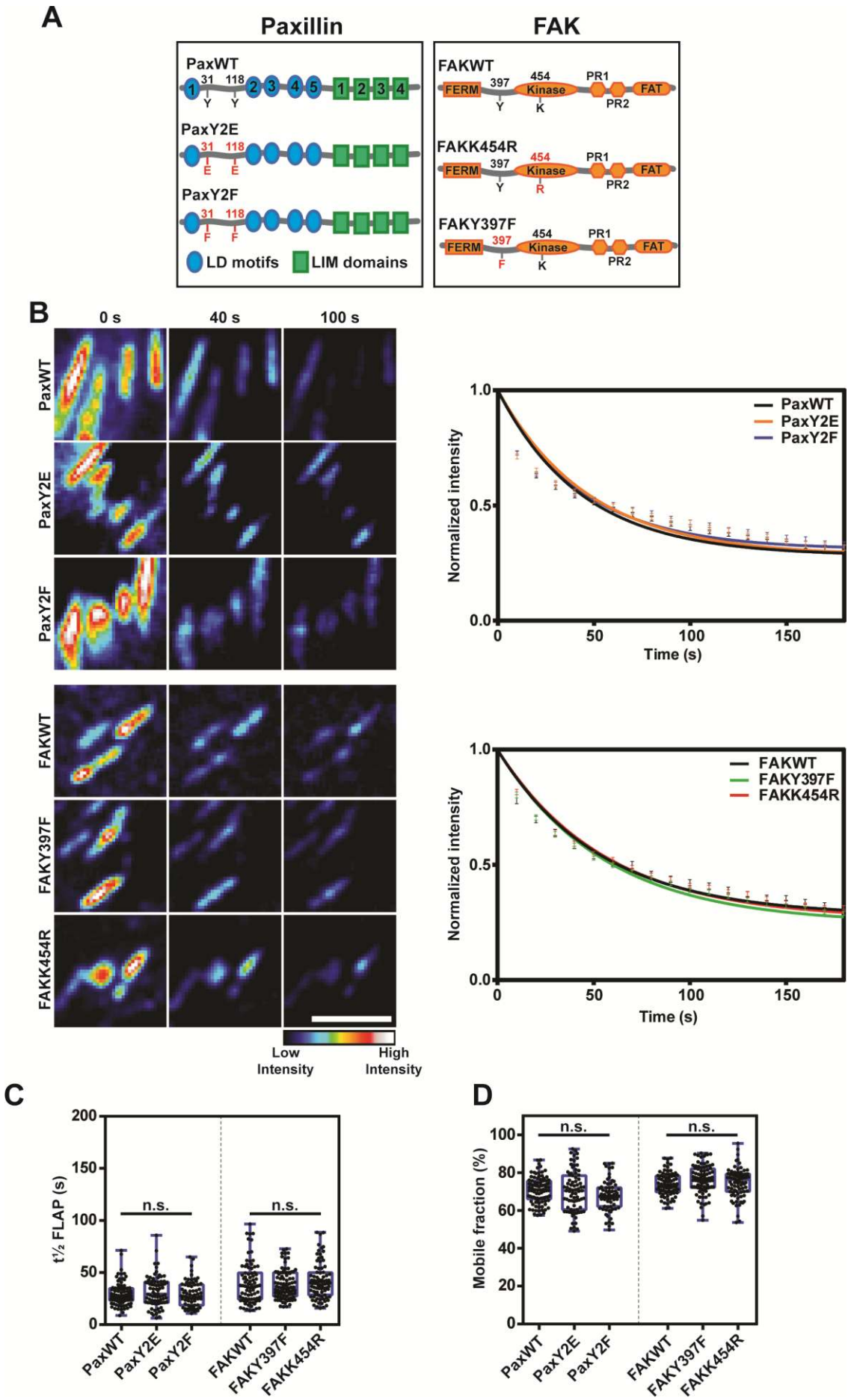

Figure 3. Phosphorylation state does not affect turnover of FAK and paxillin.

A. Schematic showing FAK and paxillin and the mutant forms that were used in the study. **B.** Representative time-lapse images showing the loss of fluorescence of the indicated PAGFP-tagged FA protein, following photoactivation; scale bar = 5 μm. Graphs showing the mean fluorescence loss over time, error bars are SEM. **C.** Mean t½ FLAP and F_M in NIH3T3 cells expressing the indicated FA protein and mutant constructs. Note there is no difference in turnover of the FAK and paxillin mutants. Data are pooled from 3 independent repeats, n = 71-96 FAs, Kruskal-Wallis with Dunn's multiple comparisons test, n.s. = no significant difference.

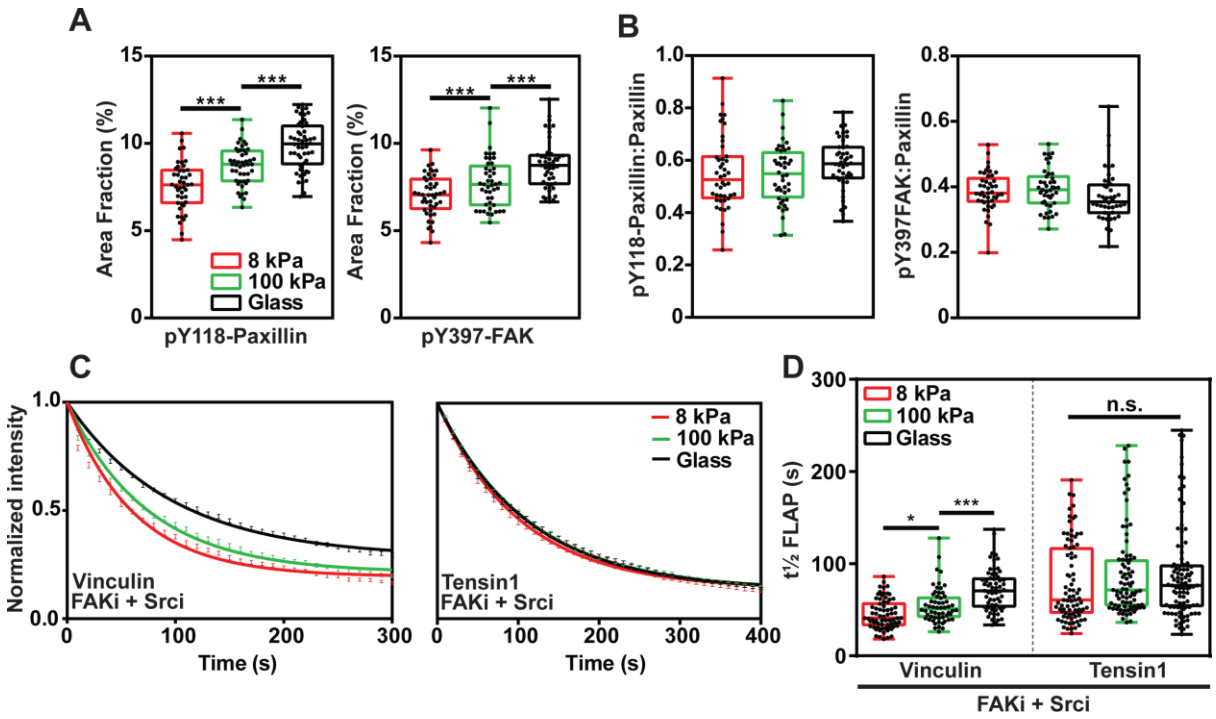

Figure 4. FAK and paxillin phosphorylation are involved in mechanotransduction

A, B. Graphs showing the percentage of the cell area that is composed of pY118-paxillin or pY397-FAK positive FAs (A) and the ratio of pY118-paxillin/pY397-FAK to total paxillin (B) in cells plated on the indicated substrates. Data are pooled from 3 independent repeats, n = 43-50 cells, one-way ANOVA with Tukey post-hoc test, *** = $p < 0.001$. **C.** Fluorescence loss curves (±SEM) of vinculin and tensin FLAP experiments performed in NIH3T3 cells plated on the indicated substrates and treated with FAKi + Srci. **D.** t½ FLAP graph shows the turnover rates of vinculin and tensin display different responses to substrate stiffness following treatment with FAKi and Srci. Data are pooled from 3 independent repeats, n = 58-75 FAs, one-way ANOVA with Tukey post-hoc test, * = $p < 0.05$, *** = $p < 0.001$.

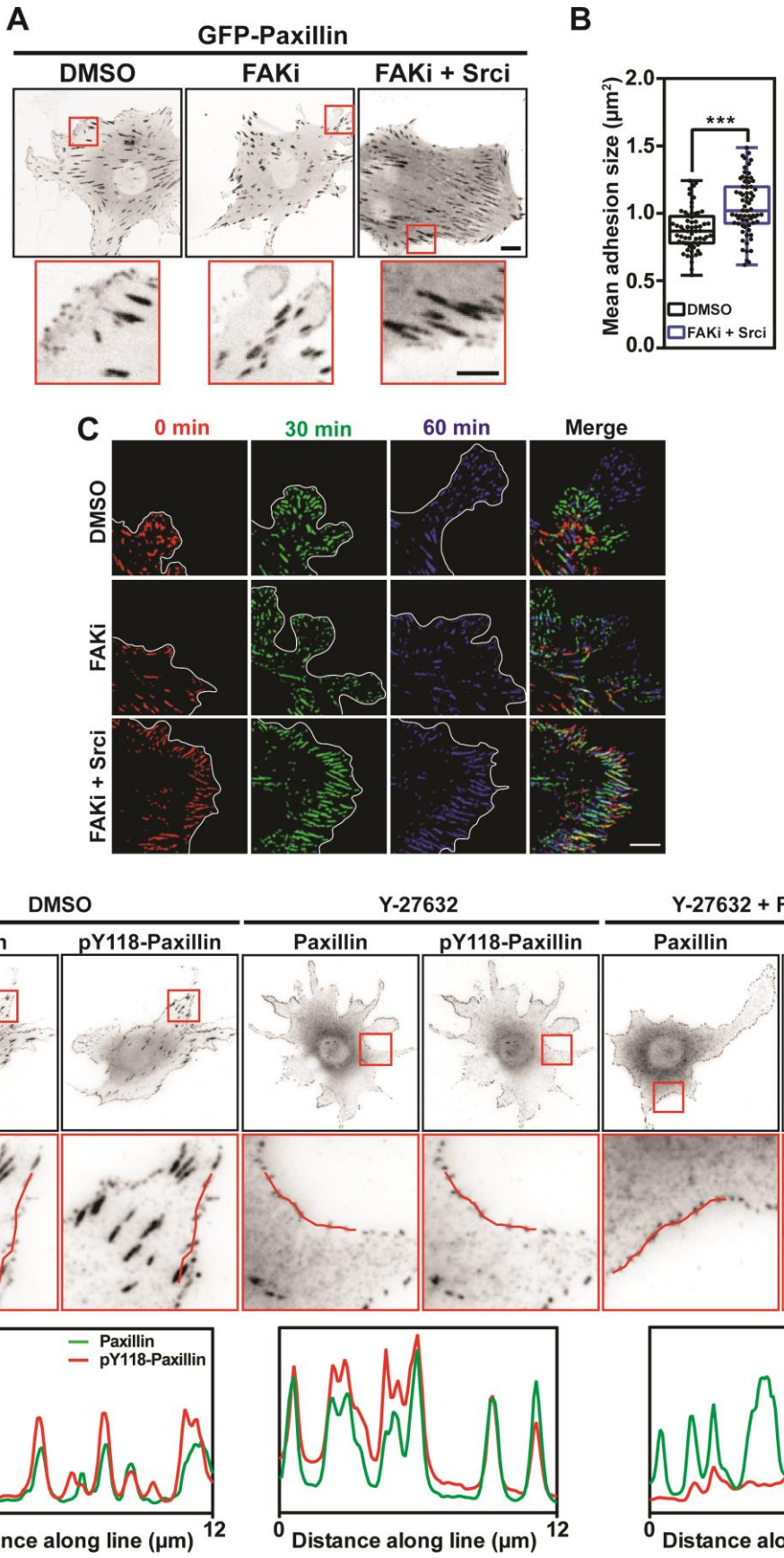

Figure 5. FAK and Src kinase activity influence FX formation and turnover.

A. Representative images showing NIH3T3 cells transfected with GFP-paxillin and treated with DMSO, FAKi or FAKi + Srci; scale bar = 10 μm. Red boxes indicate the enlarged regions (below); scale bar = 5 μm. **B.** Graph showing the adhesion size in NIH3T3 cells under indicated conditions. Data are pooled from 3 independent repeats, n = 169 cells, Students t-test, *** = $p < 0.001$. **C.** Representative time-lapse images of DMSO or drug treated NIH3T3 cells transfected with GFP-paxillin. The colored images show adhesions present at the indicated time points. Overlap in color shows the GFP-paxillin containing FA has persisted between the time points (yellow = 0 and 30 minutes, turquoise = 30 and 60 minutes, white = all three time points). Note the persistence of FAs following FAKi and Srci treatment. **D.** Representative images (above) and zoomed regions (below) of NIH3T3 cells pre-treated in suspension with the indicated drugs and co-stained for paxillin and pY118-paxillin after plating on FN-coated coverslips. Graphs show the fluorescence intensity across the indicated line. Note the presence of paxillin positive FXs even in the absence of intracellular tension and tyrosine phosphorylation. Scale bar = 10 μm (above) and 5 μm (below).

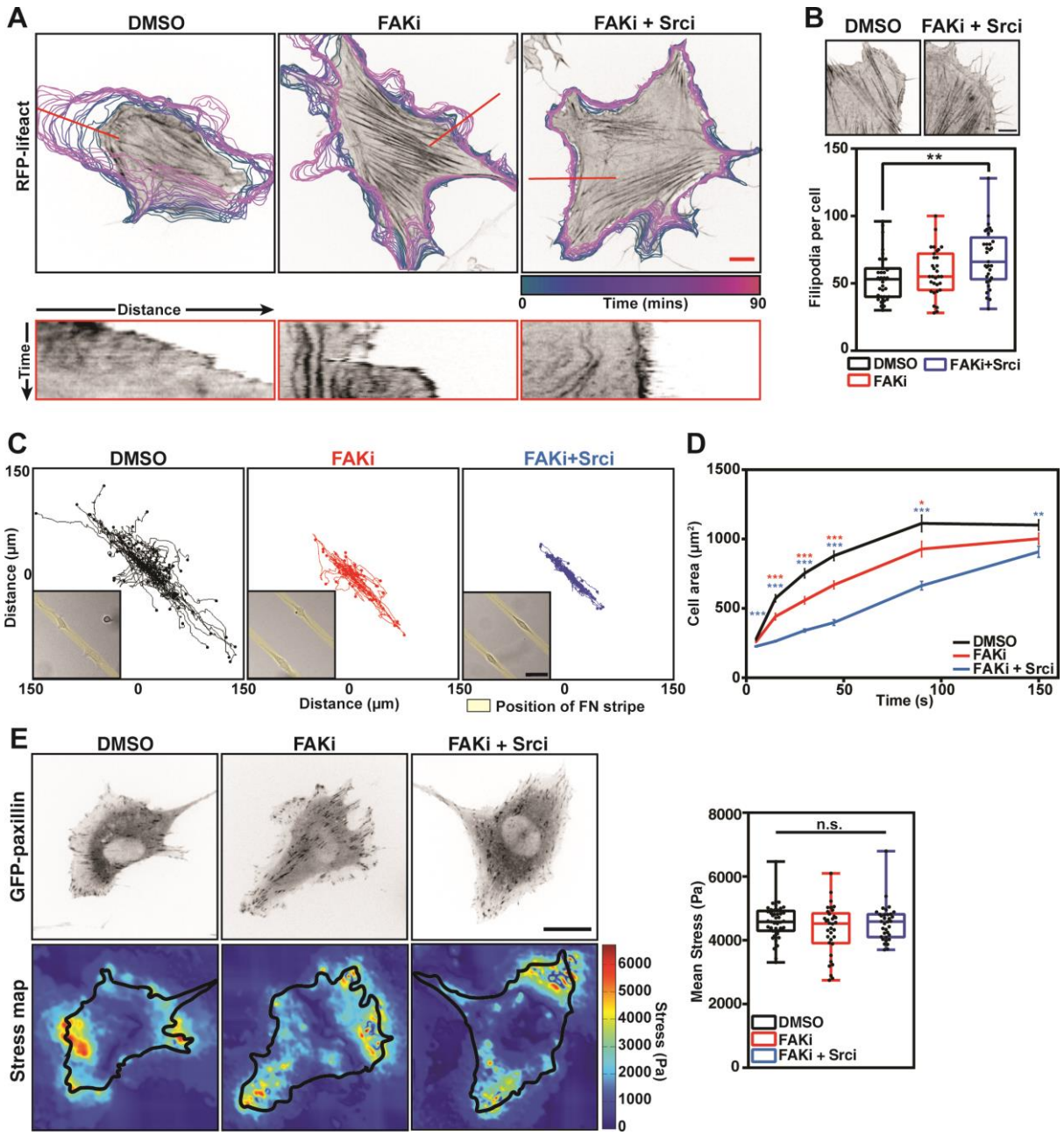

Figure 6. FAK and Src kinase activity are required for lamellipodial protrusions, cell migration and spreading.

A. Representative recordings following the indicated drug treatments of NIH3T3 cells transfected with RFP-lifeact. The color-coded outlines show the position of the cell during the course of the 90 minute movie (4 minute intervals). Kymographs (below) were taken at the indicated position (red line). Note the dramatic drop in protrusive behavior following the inhibition of FAK and Src. Scale bar = 10 μm. **B**. Quantification of number of filopodia

around the cell periphery following treatment with DMSO, FAKi or FAKi + Srci. n = 31-35 cells, one-way ANOVA with Tukey post-hoc test, ** = $p < 0.01$. **C.** Representative trajectories of cells recorded for 16 hours on 10 μm wide fibronectin stripes; images of NIH3T3 cells plated on fibronectin stripes (inset). Note the decreased migration rate of cells treated with FAKi and FAKi + Srci. **D.** Graph showing the increase in cell area over time following plating on fibronectin coated cover slips. n = 113-233 cells, one-way ANOVA with Tukey post-hoc test, n.s. = no significant difference, * = $p < 0.05$, ** = $p < 0.01$, *** = $p < 0.001$. Error bars are ± SEM. **E.** Representative cell images and stress maps of traction force microscopy. Stress maps are colored to show intensity, scale bar = 10 μm. Graph shows the mean stress of all cells analyzed. n = 34-45 cells, one-way ANOVA with Tukey post-hoc test, n.s. = no significance.

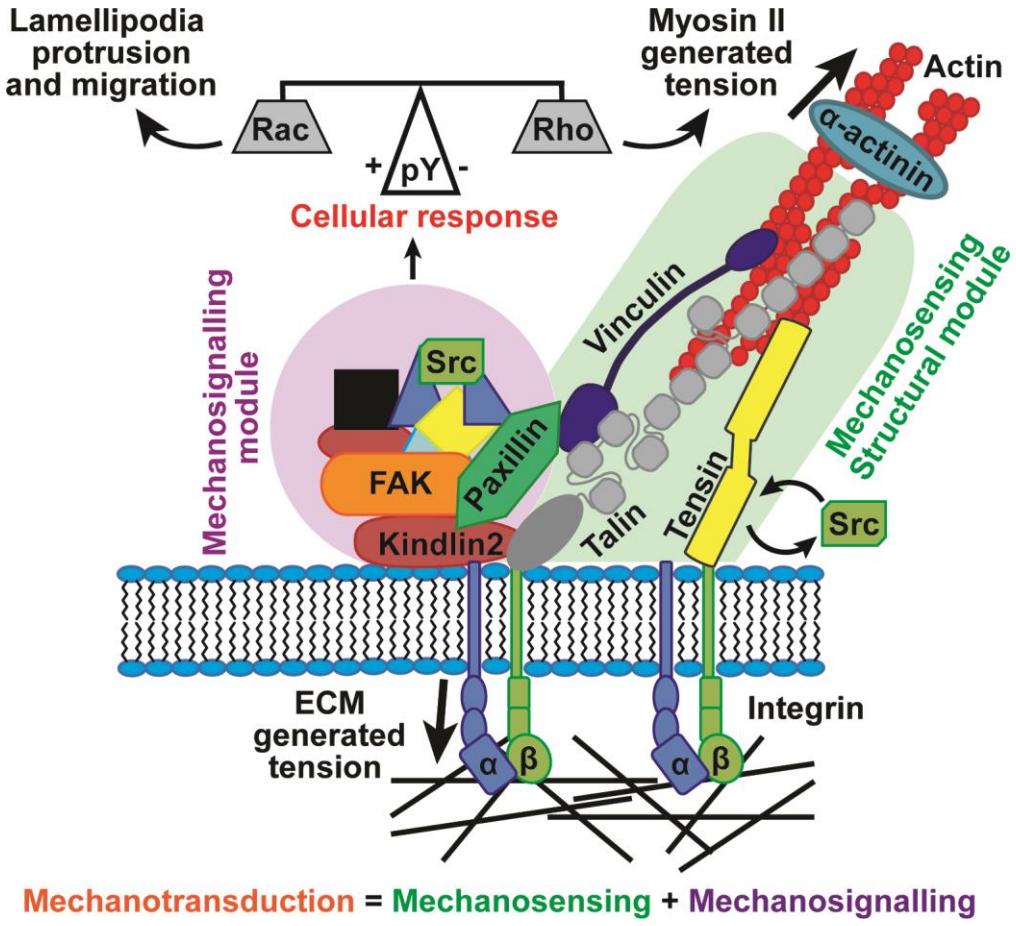

Figure 7. Model of mechanotransduction by the structural and signaling protein modules.

Proteins in the structural module, including tensin, talin and vinculin, are tightly associated with integrin and actin. These proteins sense extracellular mechanical signals by modifying their activation state and rate of turnover. This signal is transferred to the proteins in the signaling module, including FAK and paxillin, by modifying their level of tyrosine phosphorylation. The level of tyrosine phosphorylation on these proteins determines the cellular response to the mechanical signal, activating Rac to promote protrusion and migration or Rho, leading to adhesion growth and stabilization.

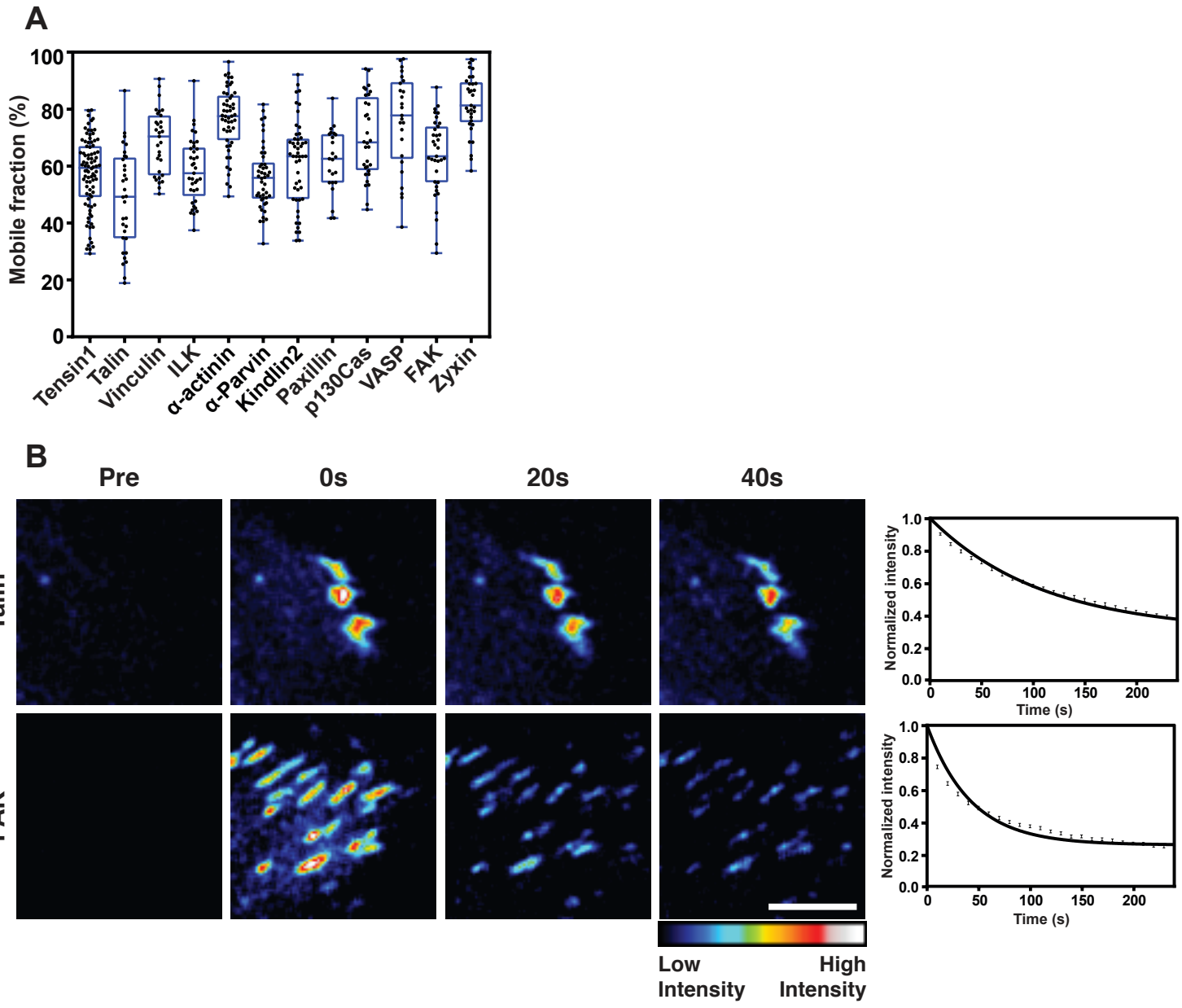

Figure S1

A. Mean mobile fraction (F_M) values for the indicated FA proteins in NIH3T3 cells. **B.** Representative time-lapse images showing fluorescence loss after photoactivation of NIH3T3 cells transfected with PAGFP-tagged talin and FAK. Images are coloured to represent fluorescence intensity. Graphs show the average fluorescence recovery curves for all recorded FAs, error bars are SEM. Scale bar = 5 µm. **C.** Graphs showing the mean t½ FLAP and F_M values for the indicated FA proteins in NIH3T3 cells. n = 66-177 FAs. **D.** Graph showing the correlation between fluorescence intensity post-photoactivation and t½ FLAP for cells expressing PAGFP-paxillin. Note that the initial fluorescence intensity, which represents protein expression level, has not effect of rate of protein turnover. Correlation determined using Pearson's correlation, p = 0.53, n.s. = no significant correlation, n = 56 FAs. Equivalent results were seen for all constructs used (data not shown).

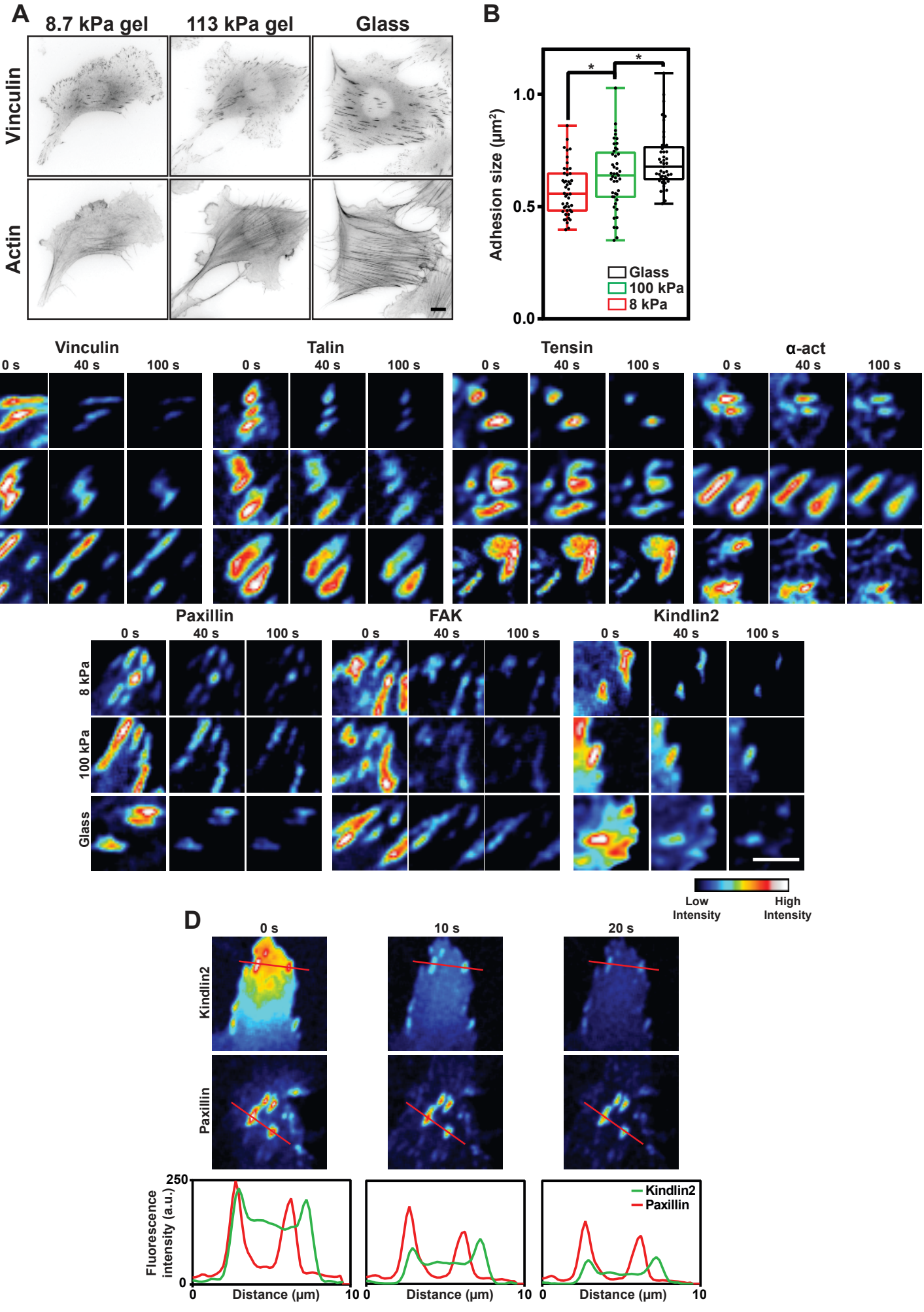

Figure S2

A. Representative images showing NIH3T3 cells plated on 8 kPa and 100 kPa polyacrylamide (PAA) gels and glass (~1 GPa) and fluorescently labelled for vinculin and actin. **B.** Graph showing the quantification of adhesion size on the different substrates. Note the increase in FA size as the substrate stiffness increases. Data are pooled from 3 independent repeats, n = 45 cells, significance determined by one-way ANOVA with Tukey post-hoc test, * = $p < 0.05$. **C.** Representative time-lapse images of FLAP experiments performed in NIH3T3 cells plated on FN-coated 8 kPa and 100 kPa polyacrylamide (PAA) gels and glass; scale bar = 5 μm. **D.** Representative images of FLAP experiments in NIH3T3 cells plated on FN-coated glass. Note the high fluorescence intensity of kindlin2 in the membrane surrounding photoactivated FAs, compared to paxillin for the first 20 s post-activation. Graphs show the fluorescence intensity along the indicated line.

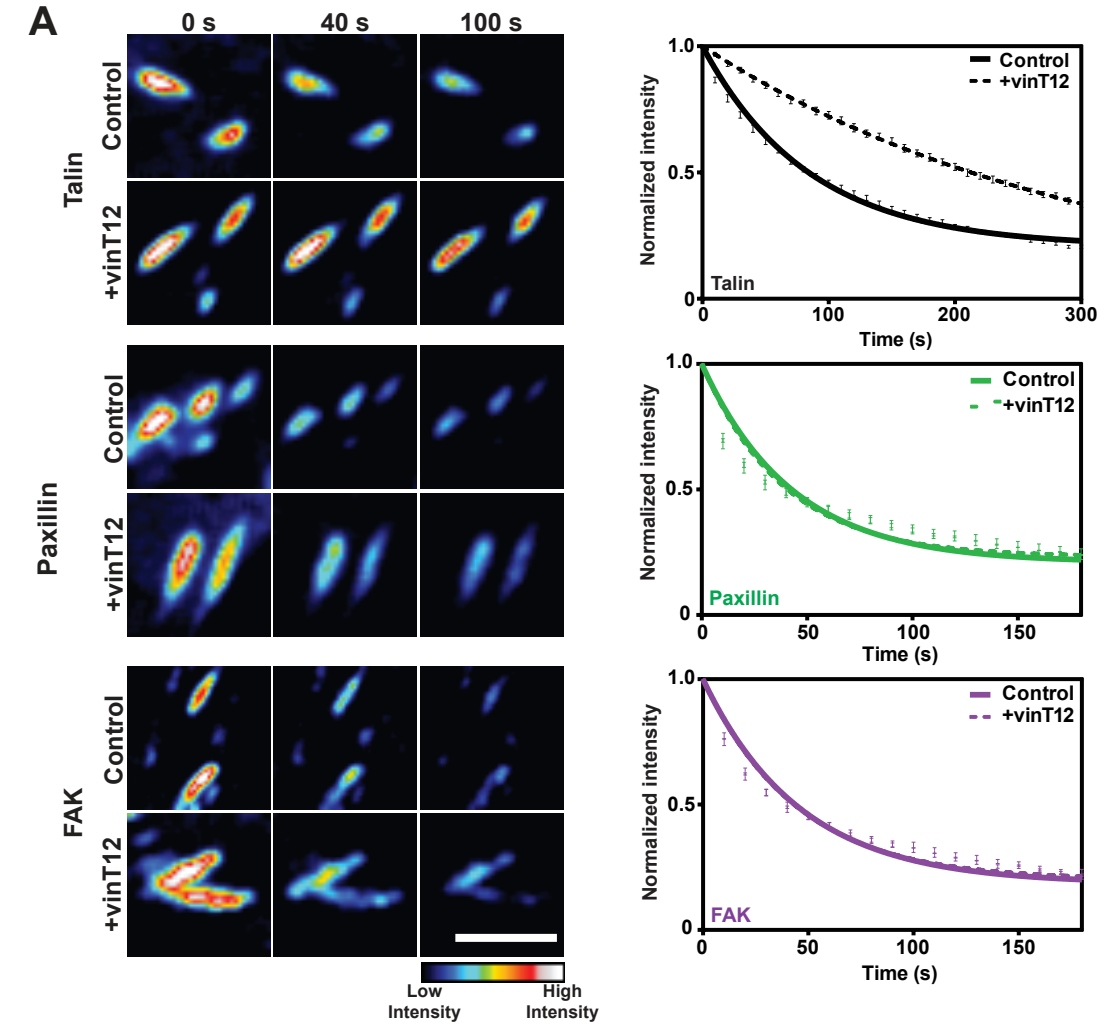

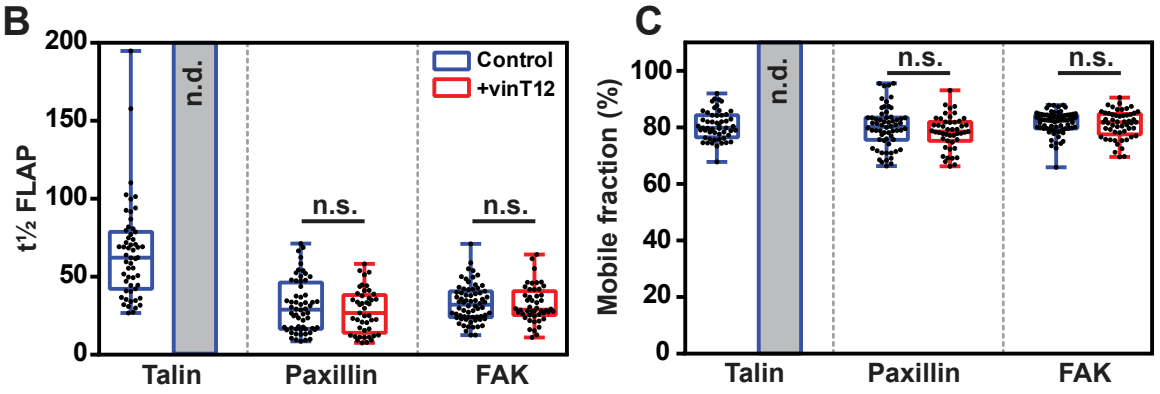

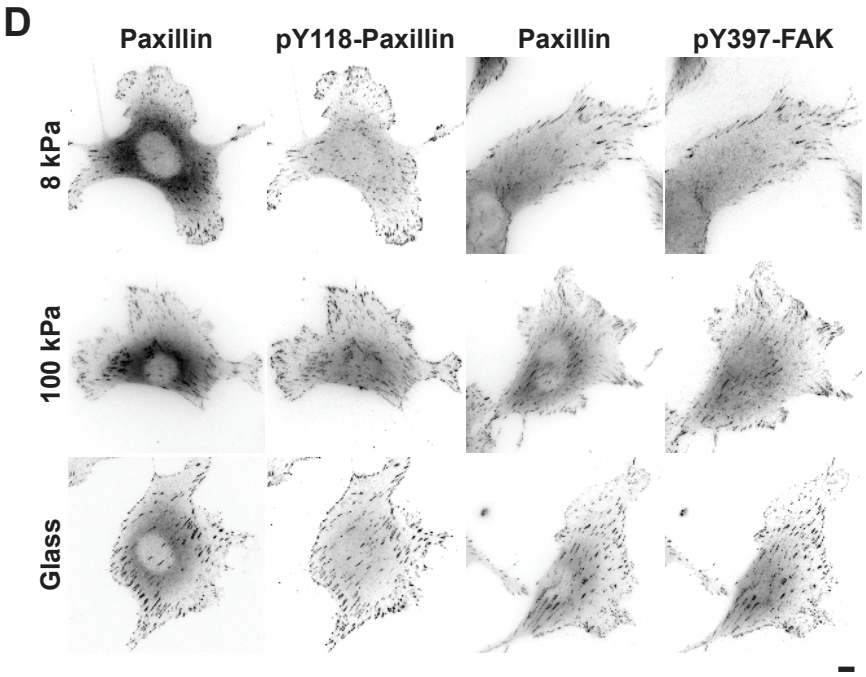

Figure S3

A. Representative time-lapse images and mean FLAP curves (±SEM) of NIH3T3 cells following photoactivation of the indicated PAGFP-tagged FA protein in control cells and in cells co-expressing vinT12; scale bar = 5 µm. **B, C**. Mean t½ and F_M graphs show that the turnover of FAK and paxillin are unaffected by the presence of vinT12. Data are pooled from 3 independent repeats, n = 45-68 FAs, one-way ANOVA with Tukey post-hoc test, n.s. = no significant difference. n.d. indicates that the t½ FLAP and F_M could not be determined due to the linear nature of the fluorescence decay. **D.** Representative images of NIH3T3 cells stained for paxillin and either pY118-paxillin or pY397-FAK; scale bar = 10 µm.

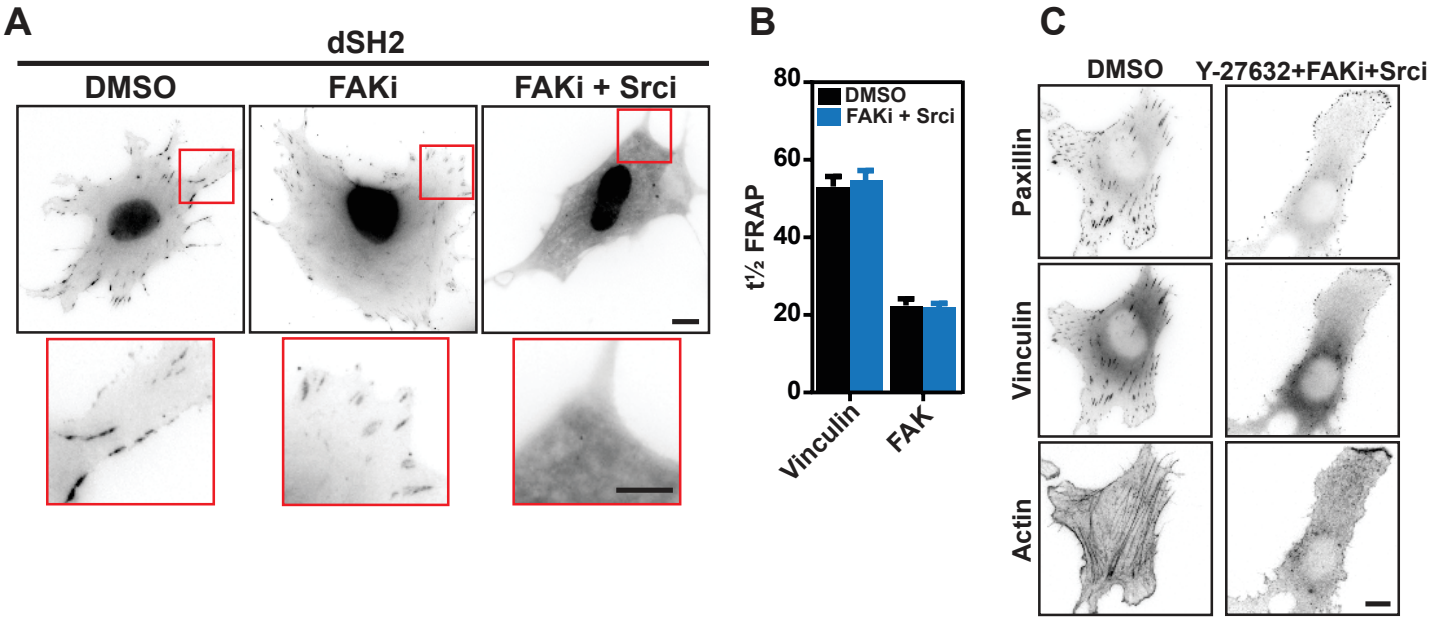

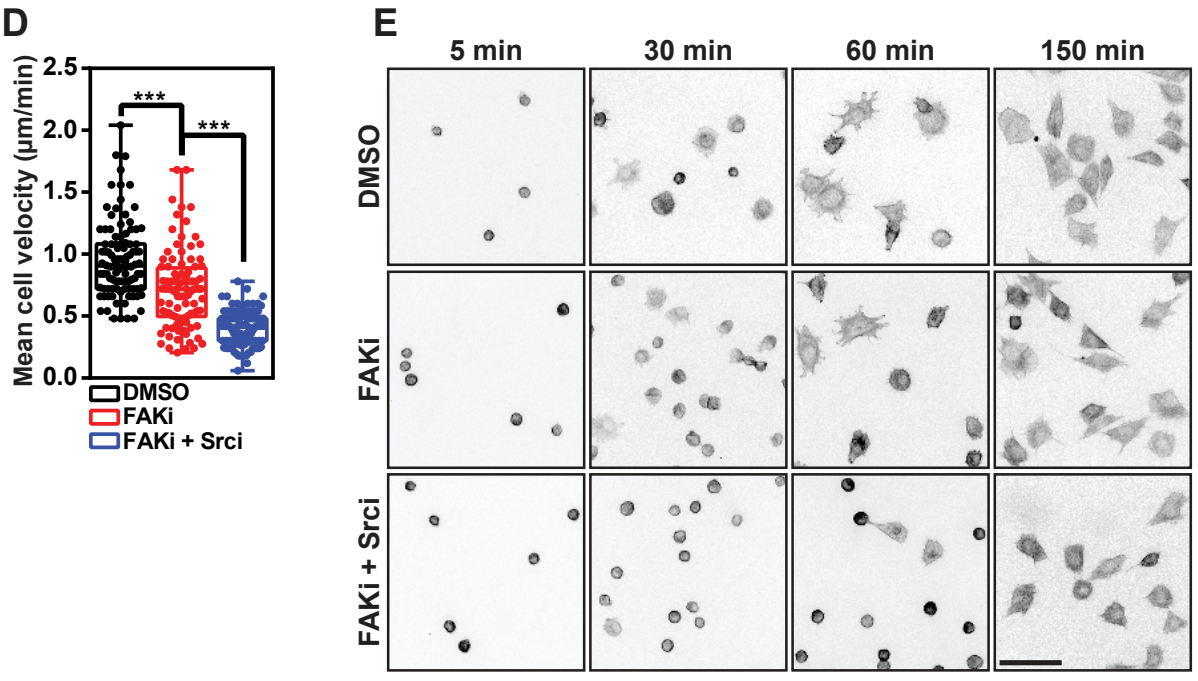

Figure S4

A. Representative images showing NIH3T3 cells transfected with YFP-dSH2 and treated with DMSO, FAKi or FAKi + Srci, scale bar = 10 μm. YFP-dSH2 is a phospho-tyrosine reporter (recognizing both phosphorylated FAK and paxillin (Ballestrem et al., 2006)). Red boxes indicate the enlarged regions (below), scale bar = 5 μm. Note the loss of dSH2 from FAs in cells treated with FAKi + Srci, indicating a loss of phospho-tyrosine from these structures. **B.** Mean t½ FRAP graph shows the turnover of FAK and vinculin are unaffected by FAKi + Srci, error bars are SEM **C.** Representative images of NIH3T3 cells pre-treated in suspension with the indicated drugs and plated on FN-coated coverslips. Note the presence of paxillin and vinculin in FXs, even in the absence of both intracellular tension and tyrosine phosphorylation. Scale bar = 10 μm. **D.** Graph showing the quantification of velocity of NIH3T3 cells plated on fibronectin stripes and imaged for 16 hours. n = 96-106 cells, significance determined by one-way ANOVA with Tukey post-hoc test, *** = $p < 0.001$. **E.** Representative time-lapse images of NIH3T3 cell spreading following pre-treatment with the indicated drugs and plated on fibronectin coated coverslips at t = 0 min. Scale bar = 50 μm.

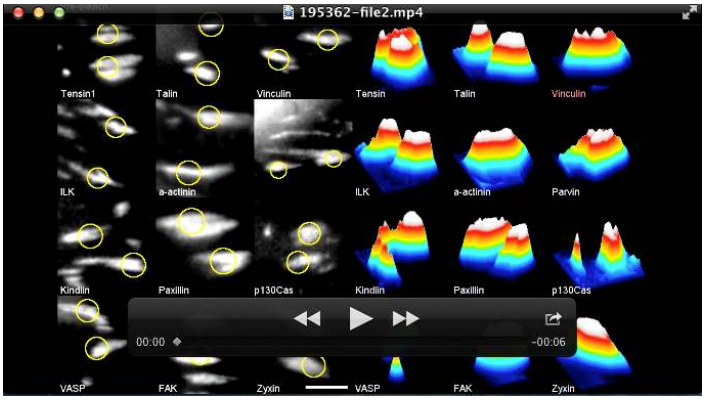

Movie S1. Related to Figure 1. Recording of FRAP experiments in NIH3T3 cells expressing the indicated core FA proteins.

The video shows FRAP in NIH3T3 cells transfected with the indicated GFP-tagged FA protein. Note the large difference in turnover rate that exists between the indicated protein modules. Images were taken every 10 seconds for 5 minutes following photobleaching. Images are played back at 5 frames/s. Scale bar represents 2 μm.

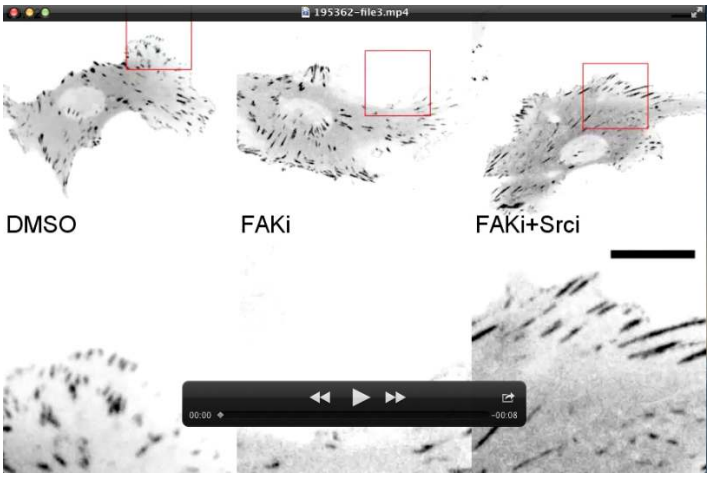

Movie S2. Related to Figure 6. Time-lapse recordings of FX formation in NIH3T3 cells treated with DMSO, FAKi or FAKi + Srci.

The video shows NIH3T3 cells transfected with GFP-paxillin and treated with the indicated drugs. The below panel shows and the enlarged region indicated in the above panel (red boxes). Newly formed FXs at the cell periphery are indicated by the red arrows. Note the difference in FA formation in cells treated with DMSO compared to cells treated with FAKi + Srci. Images were taken every 2 minutes for 90 minutes. Images are played back at 5 frames/s. Both scale bars represent 10 μm.

Movie S3. Related to Figure 7. Time-lapse recordings of cell membrane protrusive activity in NIH3T3 cells treated with DMSO, FAKi or FAKi + Srci.

The video shows NIH3T3 cells transfected with RFP-lifeact and treated with the indicated drugs. Note the difference in polarised lamellipodia protrusions between the control (DMSO) and drug treated cells. Furthermore, note the increase in peripheral filipodia in the drug treated cells, particularly evident in cells treated with FAKi + Srci. Images were taken every 2 minutes for 90 minutes. Images are played back at 7 frames/s. Scale bar represents 10 μm.